

# Physical phenomena in new organic conductors

L. P. Gor'kov

*L. D. Landau Institute of Theoretical Physics, Academy of Sciences of the USSR, Chernogolovka, Moscow District*

Usp. Fiz. Nauk **144**, 381–413 (November 1984)

Recent theoretical and experimental results on new synthetic metals—Bechgaard's salts—are reviewed. Superconductivity has been observed in these organic compounds for the first time. Furthermore, these materials exhibit such a variety of new and unusual physical properties that research on them is opening up a new branch of solid state physics.

## TABLE OF CONTENTS

1. Introduction.....	809
2. Summary of some theoretical results.....	810
3. The $(\text{TMTSF})_2\text{X}$ compounds.....	811
4. Low-temperature phase diagram.....	812
5. The characteristic of the $(\text{TMTSF})_2\text{X}$ compounds.....	812
6. Magnetic phase.....	815
7. Metallic state (low temperatures).....	817
a) Magnetotransport properties. b) Calorimetric measurements. c) NMR in the transition region. d) Hall effect.	
8. Theoretical interpretation of the phase diagram.....	821
9. The fluctuation problem.....	824
10. Structure in the state density.....	825
11. Interpretation of the observed structure.....	826
12. Conclusion.....	828
References.....	828

## INTRODUCTION

The unusual aspects of physical phenomena in materials of "reduced dimensionality" have always enjoyed a warm place in the hearts of theoreticians. The transition to two dimensions (2D) or one dimension (1D) often simplifies the theoretical analysis and generates several new experimentally observable consequences. Over the past 10–15 yr reduced-dimensionality systems have become an experimental reality: helium films, interface phenomena (in, say, heterogeneous semiconductor structures), and multilayer compounds of the chalcogenides of transition metals—all these are examples of 2D systems. The trichalcogenides of the same transition metals, organic conductors, and organic superconductors are examples of substances in which 1D properties are dominant. In this paper we will review the properties of the quasi-1D systems, more concretely, the physical phenomena in the so-called  $(\text{TMTSF})_2\text{X}$  organic superconductors<sup>1)</sup> (Refs. 1 and 2).

The search for superconductivity in an entirely new class of materials, organic materials, was in fact the stimulus for experiments in this field, primarily after Little's suggestion<sup>3</sup> that the critical temperature for superconductivity in such compounds might prove especially high because of so-called exciton mechanisms. In a nutshell, the one-dimensionality of the properties of organic conductors results from

<sup>1)</sup>TMTSF is tetramethyltetraselenafulvalenium, and X is one of various anions.

their following structural features: large planar molecules packed in stacks (or chains) so that the overlap of the electron wave functions along the stacks is large, while that between the molecules of different stacks is smaller by orders of magnitude. The effort to synthesize high-quality crystals ran into formidable experimental difficulties, which of course would not have been overcome so rapidly if there had not been this motivation of synthesizing new superconducting materials. The particular features of the superconducting state itself in these materials will be touched on only briefly in this review (see the parallel review by Buzdin and Bulaevskii). Our purpose in the present review is to show that these compounds constitute a class of materials which exhibit a rich variety of new physical phenomena, which often have no known analogs, and are consequently entities of great interest for solid state physics.

The discovery of the  $(\text{TMTSF})_2\text{X}$  compounds in 1979 was preceded by many years of research on the properties of several other organic compounds, the best-known being the TCNQ (tetracyanoquinodimethane) compounds. There is now a voluminous literature consisting of journal articles, reviews, and the proceedings of many conferences on research on specially synthesized one-dimensional (or quasi-one-dimensional, Q1D) materials. We will frequently be referring the reader to the review by Jerome and Schulz,<sup>4</sup> which is one of the most up-to-date and comprehensive reviews of organic conductors and superconductors. That re-

view contains both a history of the question and extensive factual data. Another important source of new information is the Proceedings of the International Conference on Synthetic Metals (December 1982),<sup>5</sup> which has a rich collection of factual material, although the nonspecialist will probably have difficulty in piecing together the overall picture from the brief papers there.

We will be reviewing the research results over the past two years, which may be said to lie in the domain of quantum solid state physics and the physics of low temperatures, and the evolution of thought in these fields will be reflected here.

## 2. SUMMARY OF SOME THEORETICAL RESULTS

For convenience we begin with a brief summary of the basic theoretical ideas. In the 1D approximation, under the assumption that electrons move along only one stack of molecules, the spectrum  $\varepsilon(k)$  of these electrons near the Fermi level is  $+v(k = k_F)$  and  $-v(k = -k_F)$  near the right ( $+k_F$ ) and left ( $-k_F$ ) sections of the Fermi surface (Fig. 1a; the solid and dashed lines reflect the presence of a spin: Electrons with a given momentum can have spin up or down). The energy degeneracy,  $\varepsilon(k) = \varepsilon(-k)$ , means that there are two possible mechanisms for an instability if the electrons interact with each other. Figure 1b illustrates the mechanism for a structural instability: The electron on the right (with momentum  $k$ ) is interacting with the hole on the left (of momentum  $k - 2k_F$ , with the same spin). For the Coulomb sign of the interaction, this pairing in the 1D case would always be favored and would lead to a modulation of the charge density, i.e., a charge density wave,

$$\rho_{2k_F}(x) \propto \cos(2k_F x + \varphi) \quad (1)$$

(the phase  $\varphi$  is arbitrary; the wave can glide along the chain if its period  $\pi/k_F$  is incommensurable with the period of the crystal lattice—the so-called Fröhlich mode). The distortion of the charge density in (1) unavoidably leads to a subsequent deformation of the lattice (a displacement of the ions). On the other hand, a spontaneous deformation of the lattice of the same type as in (1),

$$u_{2k_F}(x) = u_0 \cos(2k_F x + \varphi) \quad (1')$$

is favorable if we take into account the interaction of electrons with phonons, since the interaction  $d_1 u(x)$  ( $d_1$  is the strain potential) lifts the state degeneracy near  $\pm k_F$ . The deformation of the lattice in turn causes an electron charge wave (1). In either case, a gap appears in the electron spectrum (Fig. 1c). These two mechanisms, i.e., the tendency toward the formation of a charge density wave and the instability of the lattice with respect to deformation (1'), are frequently discussed from a common standpoint as a structural instability and called the Peierls instability.<sup>6</sup> Manifestations of this instability are the formation of diffuse lines near satellites on an x-ray diffraction pattern with  $k_{\parallel} = 2k_F$  and a "freezing out" of the conductivity and the magnetic susceptibility with decreasing temperature (at the transition to the insulating phase).

Figure 1d illustrates the Overhauser instability mecha-

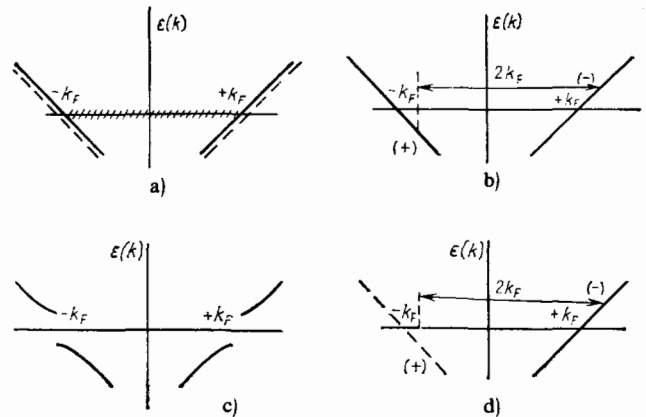


FIG. 1. Basic instability mechanisms. a—1D electron spectrum near the Fermi level (the solid and dashed lines correspond to branches of the spectrum with opposite spins); b—pairing of an electron and a hole with a vector  $2k_F$  for branches with identical spin (a charge density wave); c—the gap which appears in the electron spectrum; d—the formation of a spin density wave (the electron and hole belong to branches with different spins).

nism,<sup>7</sup> which differs from Fig. 1b in that the electron-hole pairing occurs for branches with different spin projections. A result of this instability would be a "spin density wave", i.e., an *antiferromagnetic* structure of the type in (1) and (1'). Another distinction from (1) might be a rotation of the spin vector of the structure along the chain with a period  $\pi/k_F$  (a helicoidal structure). For the  $(\text{TMTSF})_2\text{X}$  compounds discussed below, we have  $k_F = \pi/2a$ , and this question does not arise. The formation of a spin density wave would also result in the formation of a gap in the electron spectrum (Fig. 1c), so that the spin density wave would again be manifested in a dielectric transition. However, there are no structural deformations here (or they are slight), and the spin susceptibility (in a weak field) is anisotropic; only its component for the field direction along the easy axis of the spin orientation decreases.

Finally, if any electron attraction mechanism is operating there will be a Cooper instability—a pairing of electrons with momenta  $k$  and  $-k$ —which is responsible for the formation of a superconducting gap in the Bardeen-Cooper-Schrieffer (BCS) theory.

Since all these mechanisms lead to changes in the spectrum near the Fermi level (Fig. 1c), they must unavoidably compete with each other to some extent, as was first pointed out by Bychkov *et al.*<sup>8</sup>

The latter circumstance was studied in Ref. 8 in the simple 1D model of a metal, in which a leading role is played by the two electron-electron interaction constants  $g_1$  and  $g_2$ , which correspond to the scattering of electrons with a large and small momentum transfer, respectively. These two scattering processes are depicted in Fig. 2 along with yet another constant,  $g_3$ , which corresponds to spin flip and which arises only in the commensurable case,<sup>9</sup> with  $4k_F = 2\pi/a$ . After the interaction between electrons is taken into account, the effective scattering constants are found to be<sup>8</sup>

$$\tilde{g}_1 = g_1 \left(1 + g_1 \ln \frac{E_F}{T}\right)^{-1}, \quad \tilde{g}_2 = g_2 - \frac{1}{2} g_1 + \frac{1}{2} \tilde{g}_1. \quad (2)$$

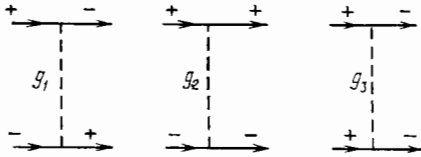


FIG. 2. The basic scattering processes in the 1D model of a metal.

If  $g_1 > 0$ , the effective interaction  $g_1$  weakens (a metallic state is possible). If  $g_1 < 0$ , superconducting fluctuations and structural deformations develop simultaneously. A tendency toward an antiferromagnetic order arises only if  $g_3 \neq 0$ . An important role is played by the sign of the combination  $g_1 - 2g_2$  ( $g_3 = 0$ ): If it is positive, the electron-electron interactions weaken the Peierls instability with respect to structural deformation, (1'). (All the results which have been derived in the 1D theory are summarized by Solov'yev.<sup>10</sup>)

The fact that the linear stacks (chains) of molecules are packed in a three-dimensional (3D) crystal requires an understanding of the role played by 3D effects. Two basic effects of this type can be cited.<sup>11</sup> The first is the interaction between electrons on different filaments (including, in particular, the 3D nature of the elastic forces, i.e., transverse dispersion or a dependence on the transverse momentum of the frequencies of all branches of the phonon spectrum). Here the electrons may be regarded as one-dimensional in the sense that the tunnel overlap of the wave functions on the different chains can be ignored. In this approximation, and in the standard band representation, the electron spectrum does not contain a dependence on the transverse quasimomentum, and the Fermi surfaces remain planar (the dashed lines in the schematic drawing of the Brillouin zone in Fig. 3a). On the other hand, the dependence of the interactions on the distance between the filaments gives rise to a transverse dispersion of the corresponding constants,  $g_1(p_\perp)$  and  $g_2(p_\perp)$ . Under these conditions the channel corresponding to a structural instability splits off from the superconducting instability. A 3D structural transition accompanied by a conversion of the electron spectrum to that characteristic of an insulator becomes possible in the system (alternately, the conversion of the electron spectrum may be only partial if the tunnel integrals are not zero). The superstructure wave vector  $\mathbf{Q}$  or, more precisely, its transverse component  $\mathbf{Q}_\perp$  [ $\mathbf{Q} = (2k_F, \mathbf{Q}_\perp)$ ] is fixed by the transverse dispersion of

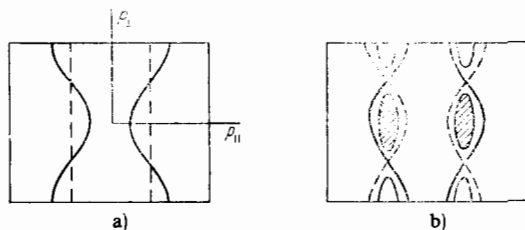


FIG. 3. Sketch of the Fermi surface in the Brillouin zone. a—One chain per unit cell. The dashed line is the planar Fermi surface in the absence of an overlap between chains; b—"hybridization" of states in a system containing one donor conducting chain and one acceptor conducting chain (the formation of electron-hole "pockets").

the electron-electron interaction forces. This is also true of a transition to the antiferromagnetic phase of the spin density wave (even if  $g_3 = 0$ ; Ref. 12) if exchange forces which depend on the spins of the electrons act between the electrons on different filaments (or if there are weaker relativistic forces between these electrons). A 3D superconducting transition cannot occur without a dispersion of the electron spectrum.

The possibility for an electron to jump from one filament to another, i.e., the transverse dispersion of the electron spectrum, is the second basic 3D effect. The Fermi surfaces are no longer planar (the solid lines in Fig. 3a). It is easy to see that a transverse dispersion of the electrons will generally have a ruinous effect specifically on the Peierls instability or the spin density wave. According to Figs. 1b and 1d, both of these instabilities occur because the tendency toward the pairing of an electron and a hole from different sides of the Fermi surface is the same for all points on this surface since both parts of it are planar (as long as the longitudinal component of the superstructure vector is  $2k_F$ ). If the parts of the Fermi surface were not planar, a given superstructure vector  $\mathbf{Q}$  (set, for example, by interaction forces) generally could not completely match the opposite parts of the surface with each other.

Figure 3a shows the electron Fermi surface for the case in which there is a single conducting chain per unit cell. A cell will very frequently contain several chains, and these chains may be of different types—electron and hole chains (this is the case in donor-acceptor compounds such as TTF-TCNQ). The tunnel overlap between chains of different types gives rise to a hybridization of the wave functions of the different filaments, with the result that closed electron-hole "pockets" can form at the right and left on the Fermi surface, at  $\pm k_F$ , as shown schematically in Fig. 3b. With increasing number of filaments per unit cell, the 3D nature of the spectrum becomes more complicated, and the "number of carriers" in these pockets decreases. Estimates of the tunnel integrals range from 50 to 200 K in different compounds. Before the discovery of the compounds of the  $(\text{TMTSF})_2\text{X}$  class, it was usually a structural transition which occurred, sooner or later, in the systems which had been studied.<sup>2)</sup> The imposition of pressure made it possible to stabilize the metallic phase. The role of the pressure is probably one of increasing the tunnel overlap integrals between chains.

### 3. THE $(\text{TMTSF})_2\text{X}$ COMPOUNDS

The effort expended on studying the properties of these compounds based on TCNQ was rewarded by more than an understanding of the nature of the ground state of these conductors and of the structural transitions which occur in them: kinetic processes which are related in some way or other to a Peierls instability. The research on these compounds resulted in the development of experimental methods for studying the physical properties of these unusual ma-

<sup>2)</sup>An exceptional case is TMTSF-DMTCNQ. See the review by Jerome and Schulz<sup>4</sup> for a discussion of these and other questions related to the properties of these systems.

materials and methods for overcoming the difficulties which result from the pronounced anisotropy, e.g., the anisotropy in the conducting properties of small crystals, their brittleness (especially in experiments involving the application of pressure), etc. Neutron and x-ray methods were developed for detecting slight structural changes which occur at low temperatures. Accordingly, when in 1979 the Danish chemist Bechgaard synthesized the new materials which were called  $(\text{TMTSF})_2\text{X}$  for short in the physics literature,<sup>1</sup> an exhaustive study of their physical properties took a bit more than two years.

A major role in these developments was of course played by the fact that superconductivity was discovered in these compounds soon after the first experiments.<sup>1</sup> Superconductivity was first discovered in  $(\text{TMTSF})_2\text{PF}_6$  under pressure<sup>2</sup> and then in  $(\text{TMTSF})_2\text{ClO}_4$  under natural conditions<sup>13</sup> ( $P = 0$ ). The rate at which experiments were carried out on this new class of "synthetic metals" in several non-Soviet laboratories is reminiscent of the proverbial California gold fever. We should say at the outset that it was the work with Bechgaard's salts, commonly called  $(\text{TMTSF})_2\text{X}$  compounds, which completed the shaping of research on Q1D conductors as a branch of solid state physics. This family (or this class) of compounds includes essentially all known states of matter: metals and superconductors, semimetals and semiconductors, antiferromagnets and antiferroelectrics or piezoelectrics. In a nutshell, these compounds exhibit all the properties which constitute the field of solid state physics. Because of all this, so many novel phenomena were discovered in these new materials that experimentalists simply have not had time to investigate their "routine properties" (e.g., their semiconducting properties).

#### 4. LOW-TEMPERATURE PHASE DIAGRAM

These new specific phenomena and properties just mentioned can be put in systematic form most easily by the phase diagram in Fig. 4, as was apparently first suggested in Refs. 4 and 14. (We have altered Fig. 4 slightly from its form in Ref. 14 to reflect some facts which have been established since the publication of that paper.)

Figure 4 is a phase diagram in the variables  $T$ ,  $P$ , and  $H$  as it could be reconstructed from data on the  $(\text{TMTSF})_2\text{X}$  compounds (Refs. 15–17 for  $\text{X} = \text{PF}_6$ ; Refs. 16 and 18–20

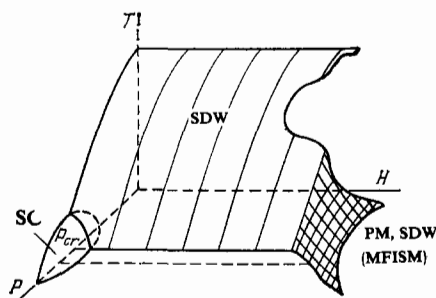


FIG. 4. General form of the  $T, P, H$  phase diagram for  $(\text{TMTSF})_2\text{X}$  compounds. The cross-hatched surface is the boundary between the metallic phase and the magnetic phase induced by the magnetic field at a pressure  $P > P_{cr}$ .

for  $\text{X} = \text{ClO}_4$ ; and Ref. 21 for  $\text{X} = \text{AsF}_6$ ). We will postpone for a bit a more detailed discussion of exactly how this diagram was obtained. The region beyond the surface designated SDW in Fig. 4 corresponds to an antiferromagnetic insulating phase; the superconducting phase (SC) occurs at magnetic fields  $H < 1$  kOe. Finally, the cross-hatched surface corresponds to the transition to the so-called magnetic-field-induced semimetallic state. As for the rest of the region (higher temperatures or higher pressures), we should classify it as the phase of an anisotropic metallic state (without going into detail at this point). In this region the behavior of the conductivity as a function of the temperature is metallic.<sup>4</sup>

We immediately note that the scale values of all the variables are quite small. This is automatically true of the superconductivity, for which we have  $T_c \sim 1$  K and  $H_{c2} \lesssim 1$  kOe. The temperature of the transition to the magnetic phase is  $T_{SDW} \approx 12$  K (for  $\text{X} = \text{PF}_6$ ); the typical pressures are  $P = 6$ –12 kbar; and the typical magnetic fields are  $H \sim 50$  kOe. As for the region of the new magnetic-field-induced semimetallic state, we note that its existence has been established reliably at temperatures to 3 K.

The magnetic phase<sup>4</sup> is a spin density wave; the state is antiferromagnetic, and the wave vector along the principal direction of  $2k_F$  is related to the 1D nature of the Fermi surfaces. To distinguish this case from the Peierls instability, one speaks in terms of the Overhauser mechanism<sup>7</sup> for the formation of an insulating state in these compounds. The fact that the insulating transition, which was first observed<sup>1</sup> in  $(\text{TMTSF})_2\text{PF}_6$ , differs in nature from the structural transition which had become quite familiar in most anisotropic (1D) conductors was the first surprise presented by these materials.

The superconducting phase in them is now identified on the basis of a variety of specific properties: the absence of a resistance, the Meissner effect, the observation of critical fields at which the superconductivity is disrupted, and—the most important point—calorimetric measurements of the specific heat, which show that the superconductivity in these compounds is a bulk effect. [The review by Buzdin and Bulaevskii covers in detail the distinctive features of the superconducting state in the  $(\text{TMTSF})_2\text{X}$  salts.]

The magnetic nature of the new phase which arises in strong fields was established from the so-called inhomogeneous broadening of the line of the NMR signal, and the semimetallic nature of this new phase is linked with the observation of the Shubnikov–de Haas effect, i.e., oscillations of the resistance as a function of the applied magnetic field, and also data on the Hall effect. The very fact that there is a *new phase* (the magnetic-field-induced semimetallic phase; Fig. 4) has now been reaffirmed by the calorimetric observation of an anomaly (a jump) in the electron specific heat.

#### 5. THE CHARACTERISTIC OF THE $(\text{TMTSF})_2\text{X}$ COMPOUNDS

To proceed further we need to briefly summarize the basic structural features of these compounds.<sup>4,22</sup> We first note that in addition to the  $(\text{TMTSF})_2\text{X}$  compounds the  $(\text{TMTTF})_2\text{X}$  compounds, isomorphous with the latter, have also attracted interest. They differ from the latter only in the

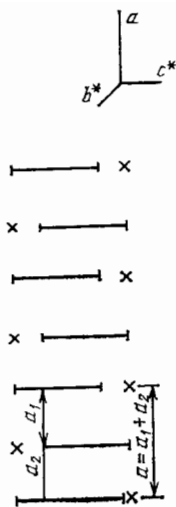


FIG. 5. Structure of  $(\text{TMTSF})_2\text{X}$ : view from the side of the chain. This sketch shows the characteristic zigzag, which forms "voids" which are filled by the anions X. The period  $a$  along the chain contains two TMTSF molecules. The general nature of the structure can be summarized as layers of stacks of TMTSF separated by planes passing through the anions.

replacement of four selenium atoms in the TMTSF molecule again by four sulfur atoms. These compounds of course fall in the same class, but the possibility of slightly varying the properties of the superconducting chain turns out to be very important, as well will see. These materials have a triclinic lattice which is comparatively close (within  $\sim 10\%$ ) to orthorhombic. The only symmetry element (at room temperature) is spatial reflection. The space group is accordingly  $P\bar{1}$ . Figure 5 is a side view of this structure, which clearly shows its basic features: a structure of linear chains of nearly plane TMTSF molecules (there are two molecules per period  $a$  along the chain); the characteristic arrangement (zigzag pattern) of transverse displacements of the molecules, which form "voids" which are filled by the anions X; and a slight dimerization of the distances between the organic molecules. The relatively simple structure is very important: There is one chain per unit cell (in the transverse direction). It can thus be expected that the electron Fermi surface will in fact consist of only two open regions. According to electrochemical arguments,<sup>1</sup> the transfer of the charge from the anions is complete ( $\text{X}^-$ ), and the electron band in the 1D band picture is half-filled<sup>23</sup>:  $2k_F = \pi/a$ . The triclinic structure of  $(\text{TMTSF})_2\text{X}$  is frequently approximated, especially in theoretical work, as orthorhombic with axes ( $a, b^*, c^*$ ) determined by the principal axes of the resistance tensor. The typical relationship between the conductivities in the corresponding directions is  $\sigma_a : \sigma_b : \sigma_{c^*} = 300 : 1 : 10^{-3}$  ( $\text{X} = \text{PF}_6$ ,  $T = 100 \text{ K}$ ; Ref. 22). The small value of  $\sigma_{c^*}$  and several other properties (e.g., the anisotropy of the magnetoresistance<sup>15</sup> and the existence of a plasma absorption edge for electromagnetic radiation polarized along the  $b$  axis<sup>24</sup>; see also Ref. 25) means that we can speak in terms of a layered structure for these compounds. The two-dimensional layers (which of course still exhibit highly anisotropic properties) in Fig. 5 correspond to vertical planes of TMTSF molecules separated by anion planes.

In a first approximation (which we will define below) the position of the anion X corresponds to a lattice inversion center. As for the anions themselves, there are many possibilities. For example, in addition to the symmetric (octahedral) anions  $\text{PF}_6$ ,  $\text{AsF}_6$ ,  $\text{SbF}_6$ ,  $\text{TaF}_6$ , and  $\text{Br}$ , there can be compounds with anions whose molecules have a lower point symmetry group: tetragonal ( $\text{ClO}_4$ ,  $\text{ReO}_4$ ,  $\text{BF}_4$ ), plane ( $\text{NO}_3$ ), and linear ( $\text{SCN}$ ) or molecules which have no point symmetry at all ( $\text{FSO}_3$ ,  $\text{CF}_3\text{SO}_3$ ). The "steric" factor is important for the  $(\text{TMTSF})_2\text{X}$  compounds: The voids or cavities formed by the zigzag pattern of the conducting chain along the  $a$  axis are quite large in comparison with the "size" of the anion as represented by the corresponding van der Waals radii (with the possible exception of  $\text{ReO}_4$ ). It is probably for this reason that noncentrally symmetric anions are disordered at room temperature. The same tetrahedral anions can, for example, generally have two orientations (an inversion), which are realized equally frequently at high temperatures. With decreasing temperature the anions become ordered, as has now been established in essentially all cases. This ordering of anions frequently plays a governing role in the nature of the ground state. In a significant number of cases the temperature at which the anions become ordered,  $T_{\text{AO}}$ , is substantially higher than the temperatures on the phase diagram in Fig. 4, so that these transitions can be distinguished from the physical phenomena in Fig. 4. The reasons why the transition to an anionic ordering turns out to be so important for the low-temperature properties can be seen from Fig. 6, where the arrows schematically show two possible orientational structures of the anions. In Fig. 6a, the period of the crystal field along the conducting chain ( $T < T_{\text{AO}}$ ) remains constant, and there is a single electron per 1D unit cell. Under these conditions there can be a metallic state, and thus there can be a superconductivity, as is in fact found to be the case for  $\text{X} = \text{ClO}_4$  when it is cooled slowly (an equilibrium R state<sup>4</sup>). In Fig. 6b this period has been doubled, with the result that we have an insulating state (for which the longitudinal Peierls component of the wave vector of the superstructure is  $2k_F = \pi/a$ ). Since we are talking about an ordering of the orientation of a charged anion, the potential created by this anion on the conducting filament is generally not small, so that there is a significant insulating gap. This interpretation is apparently supported by the particular case  $\text{X} = \text{ReO}_4$ , for which we have  $T_{\text{AO}} = 180 \text{ K}$ , and for which the energy gap is about 2000 K, according to the activation law for the conductivity.<sup>1,26</sup> Incidentally, it can be seen from

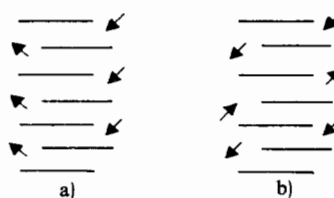


FIG. 6. a—Orientation of asymmetric anions which does not disrupt the periodicity along the chain, with the vector  $(0, 1/2, 0)$ ; b—ordering of anions which affects the conducting properties of the chain, with the vector  $(1/2, 0, 0)$ .

TABLE I.

Compound	Symmetry of anion	Transition temperature, K	Wave vector of superstructure
(TMTTF) <sub>2</sub> SCN	Linear (dipole)	160	0, 1/2, 1/2
(TMTSF) <sub>2</sub> NO <sub>3</sub>	Triangle	41	1/2, 0, 0
(TMTTF) <sub>2</sub> NO <sub>3</sub>	»	50	1/2, 0, 0
(TMTSF) <sub>2</sub> ReO <sub>4</sub>	Tetrahedron	177	1/2, 1/2, 1/2
(TMTTF) <sub>2</sub> ReO <sub>4</sub>	»	160	" "
(TMTSF) <sub>2</sub> BF <sub>4</sub>	»	40–50	" "
(TMTTF) <sub>2</sub> BF <sub>4</sub>	»	40	" "
(TMTSF) <sub>2</sub> FSO <sub>3</sub>	Tetrahedron (dipole)	87, 5	" "
(TMTTF) <sub>2</sub> ClO <sub>4</sub>	Tetrahedron	70	" "
(TMTSF) <sub>2</sub> ClO <sub>4</sub>	»	24	0, 1/2, 0
(TMTSF) <sub>2</sub> H <sub>2</sub> F <sub>3</sub>	Noncent. symm.	63	1/2, 1/2, 1/2

these figures that it is *not* the conduction electrons which determine the mechanism for the ordering of anions.

Table I, which is taken from Ref. 27 [and which includes data from Ref. 28 on (TMTSF)<sub>2</sub>H<sub>2</sub>F<sub>3</sub>], shows the most recent results on the structural studies of transitions in the ordering of asymmetric anions in (TMTSF)<sub>2</sub>X and (TMTTF)<sub>2</sub>X. It is clear from this table that the predominant transitions are those involving the structure of a 1D conducting zone, as we mentioned earlier in the case of X = ReO<sub>4</sub> (a keen observation made by Moret *et al.*<sup>27</sup> is that the volume of the unit cell changes in only one way in all cases: it doubles). Nevertheless, the consequences of the ordering of the anions are by no means in all cases as strong as they are in ReO<sub>4</sub>. The transition in (TMTSF)<sub>2</sub>NO<sub>3</sub> at  $T_{AO} = 41$  K more probably leads to an increase in the conductivity below this temperature,<sup>1,29</sup> and at  $T \approx 12$  K there is a new metal-insulator transition, which in this case is apparently magnetic in nature. In (TMTSF)<sub>2</sub>H<sub>2</sub>F<sub>3</sub> the transition at 63 K is a combination of an anionic ordering and a deformation of the nature of a charge density wave.

In many ways, this collection<sup>27</sup> of order-disorder transitions in Table I is still a lot of guesswork. The fact that (TMTSF)<sub>2</sub>NO<sub>3</sub>, for example, remains a metal below 41 K can of course be attributed without difficulty to the 3D nature of the electron spectrum,<sup>29</sup> because of which electron-hole pockets remain during a superposition of Fermi surfaces with the wave vector (1/2, 0, 0). In a phenomenological way, we could just as logically attribute the low ordering temperature  $T_{AO}$  in a noncontradictory way to a steric factor (the size) of the anion (low energy barriers). The mechanism for the ordering transition, however, remains unexplained. For example, these transitions seem at first glance to have nothing in common with the instabilities which stem from the Q1D nature of the electron spectrum: The diffuse spots ("precursors" above  $T_{AO}$ ) in x-ray structural studies are clearly of a 3D (isotropic) nature. The satellites which appear below  $T_{AO}$  are only an order of magnitude lower in intensity than the main Bragg reflections; i.e., they are orders of magnitude more intense than the satellites in typical Peierls transitions.<sup>29</sup> The transitions to the semiconducting state may also be of first order.<sup>26</sup> In general, this interpretation probably implies that these transitions result from Coulomb interactions, at least for transitions with the higher values of  $T_{AO}$ . The phenomenological theory of Ref. 30 gives

a good explanation of the parameters of the metal-semiconductor transition (for X = ReO<sub>4</sub> in the structure in Fig. 6b, for example) under the assumption that the anions form a periodic potential (of period  $2a$ ) of the Kronig-Penney type along the conducting chain for the electrons and that the energy gap which forms is wide ( $\sim 2000$  K).

A simple way to test the suggestion that the order-disorder transition is controlled primarily by the forces of the interaction between anions would be to compare the identical transitions for the isostructural compounds (TMTSF)<sub>2</sub>X and (TMTTF)<sub>2</sub>X, i.e., to test the sensitivity of these transitions to the parameters of the conducting chain. We know that the replacement of selenium by sulfur (the transition from the TMTSF molecule to the TMTTF molecule) has a quantitative effect on a characteristic such as the conductivity [the (TMTTF)<sub>2</sub>X compounds have a significantly poorer conductivity<sup>31,32</sup>], without changing the picture of events in a qualitative way. It turns out that for X = NO<sub>3</sub> and BF<sub>4</sub> the temperatures  $T_{AO}$  lie in the interval 40–50 K for both the selenium and sulfur compounds.<sup>32</sup> The same is true of (TMTSF)<sub>2</sub>ReO<sub>4</sub> ( $T_{AO} = 180$  K) and (TMTTF)<sub>2</sub>ReO<sub>4</sub> ( $T_{AO} = 160$  K) (Ref. 33). Nevertheless, for the low-temperature anionic transitions there is some difference between the selenium and sulfur compounds. It is also seen in a slightly different temperature dependence of the corresponding structural satellites.<sup>27</sup> There are thus several questions which are still difficult to answer. The most important of them is the nature of the low energy barriers and the mechanism for the order-disorder transitions. It can be seen from Table I that the temperatures  $T_{AO}$  are typically 100 K, despite pronounced differences in the symmetry and other properties of the various anions.

Another fact which we have not yet brought up is that all the differences in the nature of the ground state ( $P = 0$ ) for the compounds with asymmetric anions are erased by the application of an external pressure. The pressure required here is not only strikingly low but also approximately the same for different substances. In the (TMTSF)<sub>2</sub>X series, for example, the metallic state and the superconductivity (at  $T \sim 1$  K) prevail for both symmetric anions (X = PF<sub>6</sub>AsF<sub>6</sub>, SbF<sub>6</sub>, TaF<sub>6</sub>, etc.) and asymmetric anions (e.g., X = FSO<sub>3</sub> and ReO<sub>4</sub>) over the pressure range 6–15 kbar. A special case is (TMTSF)<sub>2</sub>ClO<sub>4</sub>, for which superconductivity has been observed at  $P = 0$  (1 bar) and which will be discussed below as a

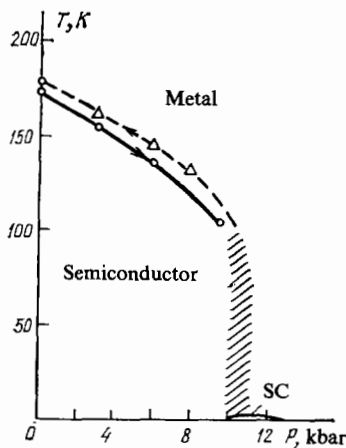


FIG. 7. Phase diagram of  $(\text{TMTSF})_2\text{ReO}_4$ . The hatching shows the "glass phase." An ordered state analogous to  $\text{ClO}_4$  can be produced in this region by slow cooling.<sup>4</sup>

typical case exhibiting all the basic properties shown on the phase diagram in Fig. 4. It turns out that the properties of this material are determined at very low temperatures by its thermal "past history" in the temperature range below 30 K (Ref. 34). During slow cooling a phase transition<sup>35</sup> occurs in  $(\text{TMTSF})_2\text{ClO}_4$  with the structural wave vector and the temperature  $T_{AO}$  listed in Table I. The ordered state [the R (relaxed) state] corresponds to a metallic phase. Rapid cooling freezes the disorder in the orientation of anions [the Q (quenched) state]. In this case the low-temperature properties of  $(\text{TMTSF})_2\text{ClO}_4$  correspond to a spin density wave.<sup>36</sup> Curiously, the same properties seem to be exhibited by the compound with  $X = \text{ReO}_4$  (Ref. 37), where the state in the hatched region in Fig. 7 had been interpreted previously<sup>26</sup> as a "metallic glass phase" (see also the results of Ref. 38 on  $\text{FSO}_3$ ). Returning to the metal-insulator transition in it, we see that even low pressures cause a change in the equilibrium electron spectrum on conducting chains.

The structural properties of these compounds discussed above, particularly the role played by asymmetric anions, were discussed in detail at a conference on synthetic metals held in France in 1982 (Ref. 5). All the results seem to indicate that there are actually only negligible differences in the properties of the conducting electrons proper, despite all the differences which seem at first glance to be substantial in the low-temperature behavior of these compounds. Weak external agents (a pressure or heat treatment) can put each of these compounds in a state whose properties are determined primarily by the characteristics of the conducting system of TMTSF molecules and which seem to vary only slightly from compound to compound.

This interpretation forces us to take another look at the compounds with centrally symmetric anions ( $\text{PF}_6$ ,  $\text{AsF}_6$ , etc.). In their original form, they exhibit a transition to a state in a spin density wave.<sup>4</sup> In roughly the same pressure interval ( $P \approx 6$ – $10$  kbar), however, they go into a metallic phase. An unexpected result of a very subtle recent analysis<sup>39</sup> of accurate structural data was the discovery that there is also a disorder (that there are also displacements) in the  $(\text{TMTSF})_2X$  compounds with octahedral, centrally symmet-

ric anions ( $X = \text{PF}_6$ , etc.; see also Ref. 40, where a disorder was observed in the arrangement of  $X = \text{TaF}_6$  anions). The existence of a magnetic phase in compounds with symmetric anions at  $P = 0$  is now being correlated to some extent with the existence of a magnetic phase in  $(\text{TMTSF})_2\text{ClO}_4$  only in the supercooled state (the Q state), where the disorder in the orientations (and, apparently, in the displacements<sup>33</sup>) of the tetrahedra is "frozen in" during rapid cooling.

In summary, the states of all the known compounds of this family seem to vary only slightly about a certain ground state which is a "base" state for all the materials. According to this hypothesis, the properties of the base state itself are related exclusively to the properties of the electronic state in the  $Q$  1D conducting system formed by the Se-Se (or S-S) contacts (we recall that the transition from TMTSF to TMTTF molecules can be seen significantly better in several properties<sup>4</sup>). From this standpoint, the compound  $(\text{TMTSF})_2\text{ClO}_4$  is of special interest in that even at zero pressure it is possible to produce in it both a metallic and a magnetic ground state by varying the degree of disorder of the anions through the appropriate choice of cooling conditions. If the existence of a magnetic phase is in fact due to disorder, then this point is difficult to interpret from the standpoint of the existing theoretical ideas. The displacement of symmetric anions from the positions corresponding to a center of inversion (with a possible subsequent lowering of their symmetry) is probably a consequence of a Jahn-Teller effect for the symmetric ions (in crystals with low symmetry).

## 6. MAGNETIC PHASE

As was mentioned earlier, the fact that the ground state of, say,  $(\text{TMTSF})_2\text{PF}_6$  corresponds to a spin density wave was extremely unexpected. In all other known cases, an obstacle to the stabilization of the metallic state and thus to superconductivity had been a structural Peierls instability accompanied by a Kohn anomaly which directly demonstrated the Q1D nature of the events (see Ref. 40, for example). It was specifically the absence of  $2k_F$  diffuse anomalies in the first x-ray structural studies<sup>40</sup> that made it possible to link the properties of the so-called insulating state in  $X = \text{PF}_6$  below  $T_N = 12$  K with the appearance of a spin density wave.<sup>41–43</sup> The most obvious method for directly detecting a spin density wave would be an experimental study of the scattering of polarized neutrons. Unfortunately, these experiments are very difficult (if only because the volume of the crystals is too small) and have yet to be carried out. Correspondingly, we do not know the exact wave vector of the spin structure. With this exception, we can assert that the antiferromagnetic nature of the phase which sets in below  $T_N$  in  $(\text{TMTSF})_2X$  with  $X = \text{AsF}_6$ , and certain other anions has been reliably established. Proof of this assertion comes from the following list of experimental facts.

During an insulating Peierls transition, the electrons "go under the gap"; i.e., the number of spin carriers decreases. Correspondingly, below the transition point there is a rapid decrease in the paramagnetic component of the magnetic susceptibility, which can be determined both from the intensity of the ESR signal and in static measurements. In

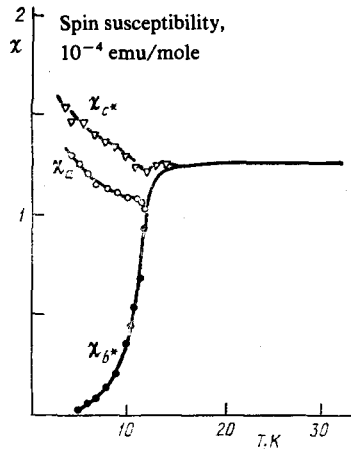


FIG. 8. Anisotropy of the magnetic susceptibility tensor below the temperature of the transition to the antiferromagnetic phase of  $(\text{TMSF})_2\text{AsF}_6$  (Ref. 44).

the first measurements with polycrystalline samples of the  $(\text{TMTSF})_2\text{X}$  class, this decrease (for the static susceptibility) was not observed down to low temperatures, although the ESR signal decreased sharply near the transition point. The situation was resolved by some more careful measurements of the anisotropy of the susceptibility<sup>44</sup> in  $(\text{TMTSF})_2\text{AsF}_6$  single crystals. Figure 8 shows the low-temperature behavior of the principal values of the magnetic susceptibility tensor in weak fields (the axes of the susceptibility tensor coincide with the principal axes of the conductivity tensor;  $a$  is the direction along the chains; and the  $b^*$  and  $c^*$  axes are close to the principal axes of the planar molecule). We see the typical behavior of the susceptibility for an antiferromagnet for which the  $b^*$  axis corresponds to the easy axis, while the  $a$  and  $c^*$  axes are an intermediate axis and a hard magnetization axis, respectively. Figure 9 shows the arrangement of spins in weak magnetic fields (Fig. 9a) and strong magnetic fields (Fig. 9b), directed along the  $b^*$  axis. This arrangement demonstrates a flipping of the spins by the field during the antiferromagnetic ordering (the so-called spin-flip transition in the  $H_{\text{SF}}$  field). Figure 10 shows experimental curves from Ref. 44 on the susceptibility in strong fields. These curves clearly demonstrate spin flipping in  $(\text{TMTSF})_2\text{AsF}_6$ . Furthermore, as we know quite well from textbooks (see Refs. 45 and 46, for example), anisotropy of the susceptibility in an antiferromagnetic phase (nonexchange terms) results from small relativistic interactions. These interactions also cause

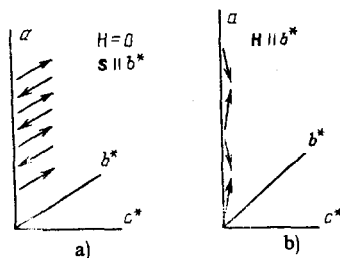


FIG. 9. Spin flipping in a magnetic field. a—There is no field, and the spins are directed along the easy  $b$  axis; b—a sufficiently strong field ( $H > H_{\text{SF}}$ ) overcomes the magnetic-anisotropy force and rotates the spins while preserving their antiferromagnetic order.

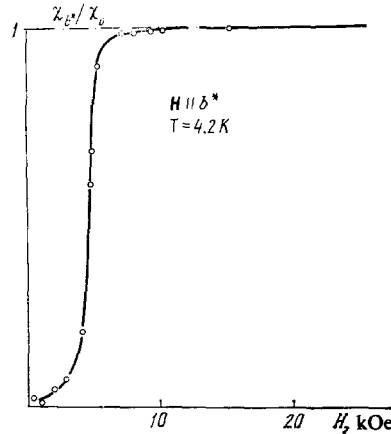


FIG. 10. Behavior of the susceptibility as a function of the magnetic field corresponding to spin flip.

the spectrum of long-wavelength excitations (magnons) to begin at a finite frequency proportional to the square root of the magnitude of the relativistic interactions. The frequencies of the antiferromagnetic resonance have been measured directly for  $\text{X} = \text{AsF}_6$  (Ref. 47) and  $\text{ClO}_4$  (Ref. 48) and in  $(\text{TMTSF})_2\text{Br}$  (Ref. 49); the results agree well with the strength of the  $H_{\text{SF}}$  field (the standard model of localized spins was used for an interpretation in Ref. 47).

Finally, the existence of static magnetic moments and an estimate of their magnitudes follow directly from NMR experiments, primarily the observation of an inhomogeneous broadening (line shift) due to local fields which arise in a spin density wave (the spin-1/2 line of the  $^{77}\text{Se}$  nucleus or of the proton<sup>50,51</sup>).

Returning to the question of the wave vector of the magnetic superstructure, we can confidently say, in view of the Q1D nature of the Fermi surfaces, that the longitudinal component is  $2k_{\text{F}} = \pi/a$ . In  $(\text{TMTSF})_2\text{X}$  there is always a strong increase in the resistance below  $T_{\text{SDW}} (\equiv T_{\text{N}})$ . With  $\text{X} = \text{PF}_6$ , for example, the system apparently remains a semimetal at low temperatures.<sup>52</sup> In  $(\text{TMTSF})_2\text{AsF}_6$  the low-temperature state corresponds to a semiconductor with a narrow energy gap of about 25 K (Ref. 21; we will not discuss asymmetric anions here because of the complications which stem from the ordering). Accordingly, the transition to the magnetic phase undoubtedly corresponds to some spin density wave with a doubled period in the longitudinal direction. The question of the values of the transverse components of the superstructure vector, however, is particularly interesting in connection with the discussion of the role of 1D effects in these compounds. The appearance of a spin density wave in these compounds might be attributed<sup>53</sup> to a very simple Overhauser mechanism: In the strong-coupling approximation, the electron spectra on the right and left sides of the open Fermi surface are,<sup>54</sup> respectively,

$$\varepsilon(\mathbf{p}) = \pm v(p \mp p_{\text{F}}) + 2t_b \cos \hat{p}b^* + 2t_c \cos \hat{p}c^*. \quad (3)$$

These spectra have the property of an ideal superposition (as in the Keldysh-Kopaev model<sup>55</sup>):

$$\varepsilon(\mathbf{p} + \mathbf{Q}) = -\varepsilon(\mathbf{p}), \quad (4)$$



where  $\mathbf{Q} = (\pi/a, \pi/b^*, \pi/c^*)$ .

The degeneracy described by (4) is lifted at low temperatures by the formation of an insulating gap which links the two parts of the Fermi surface. The question of the nature of this gap—is it due to a structural deformation or an antiferromagnetic spin wave with a vector  $\mathbf{Q}$ ?—can be answered in terms of the role played by the interaction constants in the real material.<sup>53,54</sup> If  $t_b$  is high and  $T_N$  low (various estimates yield  $t_b \sim 100\text{--}200$  K, as discussed below), then the phase transition will be three-dimensional; i.e., the overall scheme will be noncontradictory.

Another way to pose the question might be to ask whether the phase of the spin density wave is the result of instabilities embodied in the structure of the electron bands and of an interaction now in the 1D approximation (i.e., in an individual chain). That 1D effects do play a role at higher temperatures follows from the observation of weak and diffuse 1D satellites.<sup>40,29</sup> Furthermore, the insulating transition in the related compound  $(\text{TMTTF})_2\text{PF}_6$  is apparently of the nature of a charge density wave.<sup>29,56</sup>

In the search for a factor which might explain the appearance of a magnetic phase even in the 1D approximation, Barisic and Brazovskii<sup>23</sup> have called attention to the circumstance that these materials contain precisely one electron per unit cell, so that spin-flip processes can occur in them. According to our discussion in Section 2, the tendency toward the formation of a spin density wave “survives” in the presence of interactions, but it is generally suppressed by the 3D nature of the electron spectrum. A distinguishing feature of the dispersion relation in the strong-coupling approximation, (3), is that the congruence of the Fermi surfaces at low temperatures intensifies the effect if the “nesting” vector is  $\mathbf{Q} = (\pi/a, \pi/b, \pi/c)$ . As we have already mentioned, exchange interactions *between* different filaments fix the vector of the spin density wave. This vector of the structure does not contradict this interpretation. On the other hand, the conditions for the formation of a spin density wave with a vector  $(\pi/a, 0, 0)$  are *degraded* by the 3D nature of the electron spectrum, (3). The choice of this superstructure vector contradicts (4) and could be explained only in terms of a dispersion of the interactions. As we will see below, the nesting vector  $\mathbf{Q} = (\pi/a, 0, 0)$  still cannot be eliminated as an alternative possibility for an antiferromagnetic structure. In the latter case, the arguments of Ref. 23, based on spin flipping in these commensurate (1:2) conductors with spin flipping, appear to be necessary. The question of the vector of the antiferromagnetic structure will be discussed below. We also recall that, although it is a rare situation [ $(\text{TMTTF})_2\text{PF}_6$ ], there is the possibility of a transition to a state with a structure charge density wave in these compounds. Finally, as we pointed out at the end of the preceding section, there is the possibility that the formation of a spin density wave will somehow promote the presence of some structural disorder.

## 7. METALLIC STATE (LOW TEMPERATURES)

We turn now to that part of the phase diagram in Fig. 4 where pressure stabilizes a metallic state with a high conduc-

tivity. We will primarily be discussing results obtained on  $(\text{TMTSF})_2\text{PF}_6$  and  $(\text{TMTSF})_2\text{ClO}_4$ . For the latter compound the metallic phase corresponds to a relaxed (R) state even at zero pressure. Nevertheless, the actual symmetry of the R phase corresponds to the vector  $(0, \pi/b, 0)$  (Table I). At this point it is not clear to what extent this is a fundamental distinction from the case of  $\text{PF}_6$ .

We will not discuss the narrow region of temperatures and magnetic fields on the phase diagram in which a 3D superconducting phase exists. It is the metallic phase ( $H > H_{c2}$ ) with its unusual properties on which we will focus. The high conductivity ( $\sim 10^5\text{--}10^6$  S/cm), the absence of a mechanism for a residual resistance at liquid-helium temperatures, and the high magnetoresistance were the facts which led a French group at Orsay to hypothesize that superconducting fluctuations might play a role in the conductivity mechanisms for the metallic phase<sup>57,58</sup> (the question of superconducting fluctuations in a low-temperature metallic phase stabilized by pressure arose in connection with the properties of the compound<sup>59</sup>  $\text{TMTSF-DMTCNQ}$  (see the discussion in Ref. 4). This hypothesis stimulated extensive studies which have been rewarded with several extremely interesting results. At this point we turn to these results, postponing a discussion of the superconducting fluctuations themselves.

### a) Magnetotransport properties

The large positive magnetoresistance of these compounds had been discovered in Refs. 58 and 60, as we have already mentioned. A weak link in the interpretation of the phenomenon in terms of superconducting fluctuations seems to be that even in comparatively strong fields ( $> 50$  kOe) and at high temperatures the magnetoresistance  $\Delta\rho(H)/\rho_0$  exhibits no tendency toward saturation (as a function of the field), although we would expect saturation for open trajectories if the magnetic field ultimately causes a complete disruption of superconducting pairing.

A study of the anisotropy of the magnetoresistance presents another possibility for determining to what extent the electron spectrum is three- or one-dimensional. Reliable experiments on the anisotropy of  $\Delta\rho(H)/\rho_0$  can be carried out in a configuration in which the current is flowing along the  $a$  axis and the magnetic field lies in the  $(b^*, c^*)$  plane, perpendicular to the current direction. [The  $(b^*, c^*)$  plane lies  $5\text{--}10^\circ$  from the  $(b, c)$  crystallographic plane.] The anisotropy of the magnetoresistance has turned out to be extremely pronounced both at  $P=0$  in the insulating phase of<sup>61</sup>  $(\text{TMTSF})_2\text{PF}_6$  and in the metallic phase at<sup>15-17</sup>  $P=6\text{--}9$  kbar: Specifically, the magnetoresistance in strong fields ( $\sim 100$  kOe) reaches two orders of magnitude in the orientation  $\mathbf{H}\parallel c^*$  and is essentially negligible in the orientation  $\mathbf{H}\parallel b^*$ . A similar result has been found<sup>62</sup> for  $(\text{TMTSF})_2\text{ClO}_4$ . Hence we can draw the conclusion, mentioned previously, that although these compounds do exhibit 3D features (there is the possibility that orbital currents can flow), at low temperatures these compounds resemble 2D, i.e., layered, structures in terms of the properties of their electron spectrum. An important point<sup>15-16</sup> is that the magnetoresistance de-

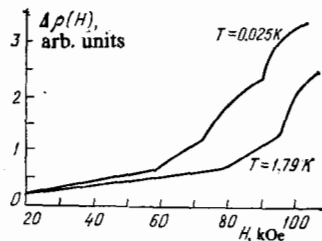


FIG. 11. Typical curves of the resistivity versus the magnetic field for  $(\text{TMTSF})_2\text{ClO}_4$  at two temperatures.<sup>64</sup>

depends on the temperature down to the very lowest temperatures. A phenomenological estimate is  $\Delta\rho(H)/\rho_0 \sim (\omega_H \tau)^2$ , where  $\omega_H$  is the "cyclotron frequency," and  $\tau$  is responsible for the effective scattering mechanism, which again indicates that there is no mechanism for a residual resistance (or that it plays only a minor role).

The most interesting results, as mentioned in Section 4, are the observation of the distinctive oscillations of the Shubnikov-de Haas type in  $(\text{TMTSF})_2\text{PF}_6$  under pressure<sup>15-17</sup> and in the R state for  $(\text{TMTSF})_2\text{ClO}_4$  (Refs. 20, 63, and 64). Figure 11, from Ref. 64, shows the increase in the resistance with the field for the latter compound; we can clearly see the distinctive behavior. Figure 12 is a typical plot of the second derivative with respect to the magnetic field versus the longitudinal resistance in  $(\text{TMTSF})_2\text{PF}_6$  under pressure.<sup>17</sup> In this compound the fields corresponding to the spikes in the derivative conform well to a periodic functional dependence on  $1/H$ . Writing the period  $\Delta(1/H)$  in the form

$$\Delta \frac{1}{H} = \frac{2\pi |e| \hbar}{cS}, \quad (5)$$

we can estimate the orbital area  $S$  to be about 1% of the cross-sectional area of the Brillouin zone.<sup>65</sup> In  $(\text{TMTSF})_2\text{ClO}_4$  the periodicity in the inverse field is not as well defined. The most interesting features of these oscillations, however, are as follows.

The oscillations are not found in weak fields,  $H < H_0$ , where  $H_0$  is some threshold field. When the threshold field is reached ( $H > H_0$ ), the oscillations appear, immediately at a substantial level. If these oscillations have the same meaning as in the Shubnikov-de Haas effect, this phenomena would indicate a sharp transition to a semimetallic phase induced by the magnetic field: The closed trajectories (or orbits) are not present at  $H < H_0$  and appear at fields  $H > H_0$ .

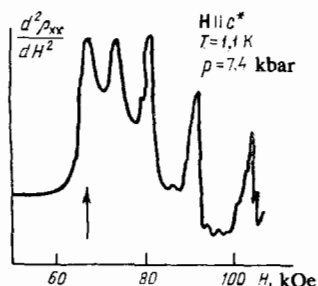


FIG. 12. Second derivative of the longitudinal resistivity with respect to the magnetic field  $H$  in  $(\text{TMTSF})_2\text{PF}_6$  under pressure.<sup>17</sup> The arrow shows the threshold field  $H_0$  above which anomalous Shubnikov-de Haas oscillations are observed.

The threshold field depends on the temperature:  $H_0(T)$  increases with the temperature in both  $\text{PF}_6$  and  $\text{ClO}_4$  (Refs. 17 and 64). The threshold-field effect is very sharp (at  $T \sim 1$  K we have  $\Delta H/H \sim 10^{-1}-10^{-2}$ ). These comments also apply to the characteristic features of the oscillations observed in the resistance. The frequency of the oscillations for example, in turn depends on the temperature (the corresponding fields increase with increasing temperature). It can be seen from Fig. 12 that the oscillations in  $\text{PF}_6$  are very narrow, by no means sinusoidal (this is a surprising result from the standpoint of the customary interpretation: the higher harmonics in the amplitude of the signal usually fall off exponentially with their index at a fixed temperature). The angular dependence of the oscillation frequency (the dependence on the field orientation) in  $\text{PF}_6$  again suggests a 2D (cylindrical) nature of the orbits (there is a  $\sec \theta$  law, where  $\theta$  is the angle between the field and the  $c^*$  axis<sup>17</sup>). In the case of  $(\text{TMTSF})_2\text{ClO}_4$ , this assertion cannot be made as confidently.<sup>63</sup>

A circumstance which appears important is the approximate periodicity of the oscillations along the  $(1/H)$  scale [at least for  $(\text{TMTSF})_2\text{PF}_6$ ]. On the one hand, this result implies that the phenomenon is of an orbital nature; on the other hand, in an interpretation in terms of Shubnikov-de Haas oscillations this result would mean that the semimetallic phase is clearly formed and that the orbits are finite immediately at  $H > H_0$  (the field  $H_0$  itself in  $\text{PF}_6$ , for example, conforms fairly well to the series of oscillatory peaks; see Fig. 12). We might note that calorimetric measurements (discussed below) speak in favor of a continuous phase transition (a second-order transition) from a metallic phase to a semimetallic state.

#### b) Calorimetric measurements

Figure 13 shows some unique measurements of the temperature dependence of the electron specific heat, which clearly indicate a continuous phase transition (at  $P = 0$  and  $H = 63$  kOe,  $T_c \approx 1.4$  K) [unique in the sense that so far these results have been observed only for  $(\text{TMTSF})_2\text{ClO}_4$ ; Refs. 14, 66, and 67]. The size of the jump in the electron specific heat cannot be determined because of experimental difficul-

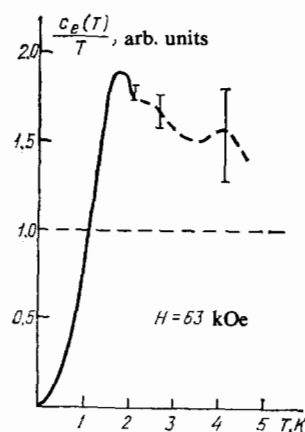


FIG. 13. Calorimetric measurements<sup>14</sup> which reveal the jump in the electron specific heat as a function of the temperature at a fixed magnetic field [for  $(\text{TMTSF})_2\text{ClO}_4$ ].

ties in distinguishing the phonon contribution at  $T \gtrsim 2$  K. The experimental results do not rule out the possibility that the behavior of  $C_e(T)$  is somewhat more complicated than linear at these temperatures.

### c) NMR in the transition region

The intensity of the NMR line for spin-1/2 nuclei ( $^{77}\text{Se}$  or  $^1\text{H}$ ) evidently obeys a Curie law with decreasing temperature ( $\chi_{\text{nuc}} \propto T^{-1}$ ). The appearance of electron magnetic moments leads to the appearance of fields (of a hyperfine nature) at the nucleus which shift the resonant frequency and thus sharply reduce the intensity of the signal. This method ("inhomogeneous line broadening") thus makes it possible to detect magnetic structure (if it exists) in the new phase.

At the same time, magnetic fluctuations increase in importance near the transition, affecting the line width and the characteristic  $T_1^{-1}$  extracted from it (the rate of "homogeneous" relaxation). Both these phenomena have demonstrated their effectiveness (in combination with other methods) in deciphering the antiferromagnetic nature of the "insulating" phase of  $(\text{TMTSF})_2\text{PF}_6$ , etc., at  $P = 0$  (see the discussion above and the discussion in Ref. 4). This method was used in Ref. 68 [for  $(\text{TMTSF})_2\text{PF}_6$  under pressure at  $H \sim 60$  kOe] and in Refs. 19 and 20 [for  $(\text{TMTSF})_2\text{ClO}_4$ ] as a tool for proving the magnetic nature of the "semimetallic" phase induced by a magnetic field. Figure 14, for example, demonstrates the decrease in the intensity of the NMR signal from the  $^{77}\text{Se}$  nucleus in a field  $H = 73.9$  kOe, which is evidence of a transition with a temperature  $T_N = 2.15$  K.

### d) Hall effect

The Hall effect has recently been studied<sup>69,70</sup> at both low and high fields in  $(\text{TMTSF})_2\text{ClO}_4$ , in which it is a comparatively simple matter to measure the off-diagonal components of the conductivity tensor because the experiments can be carried out at atmospheric pressure. The primary purpose of the measurements of the Hall constant at low fields in the metallic phase (the R state) was to confirm our understanding of the nature of the electron spectrum. Since there is only one conducting chain of TMTSF stacks per unit cell in the  $(\text{TMTSF})_2\text{X}$  salts [we are not considering the period doubling with the vector  $(0, 1/2, 0)$ ], the Fermi surface of the

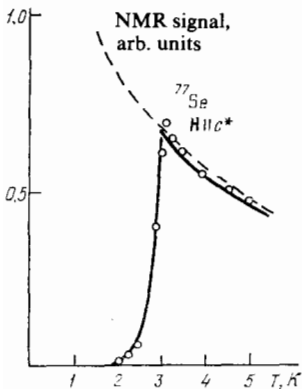


FIG. 14. Observation of a transition to a new phase based on a decrease in the intensity of the NMR signal. The dashed lines correspond to the Curie law for nuclear spins.<sup>4</sup>

Q1D metal would correspond to two open quasiplane regions at  $p_{\parallel} = k_F$  and  $p_{\parallel} = -k_F$ , respectively. This is a very important point: In other compounds (i.e.,<sup>59</sup> TMTSF-DMTCNQ) the hybridization of states on the donor and acceptor filaments is capable of producing closed pockets without any metal-insulator transitions (Fig. 3b). That there are no pockets in the metallic phase of  $(\text{TMTSF})_2\text{PF}_6$  under pressure follows immediately from the absence of Shubnikov-de Haas oscillations in low magnetic fields,  $H < H_0$  (with the reservation that small groups simply might not be visible in the technically complicated experiments with small crystals<sup>16</sup>). Measurements<sup>69</sup> of the Hall constant in  $(\text{TMTSF})_2\text{ClO}_4$  in weak fields ( $H < 40$  kOe) have completely confirmed the argument that there are two open parts of the Fermi surface: The Hall component of the voltage depends linearly on the magnetic field, and the number of carriers determined by the Hall constant agrees within the experimental error with the number which would be expected from the stoichiometry of the compound (one electron or, more precisely, one hole per unit cell). Measurements of the Hall effect in strong fields<sup>69,70</sup> not only reproduce several aspects of the behavior of the metallic phase in a field which have been observed previously on the basis of oscillations of the magnetoresistance but also demonstrate some interesting new features of the phenomenon. Figure 15 compares<sup>69</sup> the behavior of the longitudinal resistance (the scale at the left) and the Hall component of the resistance (the scale at the right; at  $H < 40$  kOe, the effect is determined by the stoichiometric number of carriers,  $n \sim 10^{21} \text{ cm}^{-3}$ , so that it is too small in this particular scale). The results of Ref. 70 now make it possible to draw conclusions about the features in the Hall effect in  $(\text{TMTSF})_2\text{ClO}_4$  at fields up to  $H \approx 22$  T. The measurements of Refs. 69 and 70 were carried out at temperatures to  $T \sim 0.1$  K.

According to Fig. 15, at  $H > 40$  kOe the Hall effect increases substantially and then decreases slightly and stays on a plateau up to  $H \sim 50$  kOe; then it rises sharply and reaches another plateau at  $H \sim 60$  kOe. A renewed rapid increase leads to a very well-defined plateau up to the highest fields in the experiments of Ref. 69 ( $\sim 80$  kOe).

In Ref. 70 ( $T = 0.08$  K) the steps in the plot of the Hall component of the resistance  $\rho_{xy}$  are preceded, beginning at  $H \approx 60$  kOe, by some slightly smaller structural features at weaker fields, near the field values in Ref. 69. Between 32.5 and 80 kOe, five structural features are found in  $\rho_{xy}$ , spaced

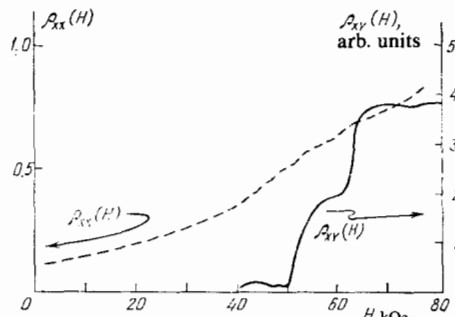


FIG. 15. Longitudinal and Hall components of the resistance as functions of the magnetic field. This behavior implies a series of phase transitions with increasing field.<sup>69</sup>

roughly periodically along the  $1/H$  scale with a frequency  $\sim 23$  T. These steps and the plateaus in  $\rho_{xy}$  are observed in Ref. 70 even at higher temperatures. While between 0.52 and 1.5 K there is a saturation in  $\rho_{xy}$  in the strongest fields (between 12 and 22 T), the dependence on the field is restored at higher temperatures. On the whole, the Hall component of the resistance decreases with increasing temperature (at a given field).

The two-dimensional (layered) nature of these compounds makes it very tempting (as was pointed out in Refs. 69 and 70) to attribute the plateaus observed in the behavior of the Hall component of the resistance to a quantum Hall effect in 2D structures (we recall that in a strong magnetic field the electrons in planar heterostructures, completely filling the Landau level, make a contribution to the Hall conductivity which is expressed in terms of a combination of universal constants,  $e^2/h$ ; Ref. 71). The estimates of Refs. 69 and 70 do not contradict this interpretation quantitatively.

Although effects associated with a quantization of the Hall constant cannot be completely ruled out, some other mechanisms are required to explain the structural features in the Hall component of the resistance in the field. For example, the voltages characterizing, say, the plateaus on the two sides of the jump in  $V_H$  at  $H \sim 60$  kOe (Fig. 15) depend on the temperature. We might add that it appears from the same figure that the longitudinal resistance in the plateau has no significant tendency to decrease, as we would expect on the basis of the present understanding, which has the plateau in the Hall voltage corresponding to the position of the chemical potential of an electron in the energy region of localized states.

An interpretation proposed in Refs. 69 and 70 for the features observed in the Hall effect in  $(\text{TMTSF})_2\text{ClO}_4$  is that with increasing field there is not simply a transition to a new, magnetic, phase but an entire series of such transitions. In these transitions, a semimetallic phase (a spin density wave) forms first (when the transition is approached from the side of lower magnetic fields), with a certain "pocket size." During subsequent transitions with a further increase in the field, the sizes of the pockets decrease. This interpretation might explain the origin of the jumps in the Hall constant (or the regions in which  $\rho_{xy}$  increases sharply with the field). In this interpretation, the behavior of  $\rho_{xy}$  would be as sketched in Fig. 16: a series of linear regions whose projections intersect the origin. The experimental data available are quite far from this ideal picture. However, if we nevertheless adopt the conventional interpretation that  $\rho_{xy}(H)/H$  is a measure of the reciprocal of the number of carriers then the data on

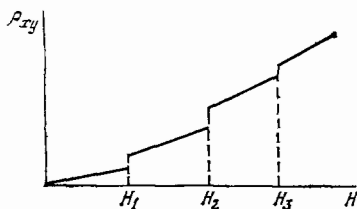


FIG. 16. Behavior expected for the Hall component of the resistance tensor as a function of the field if the number of carriers in the semimetallic phase changes abruptly at the fields  $H_1$ ,  $H_2$ , etc.

the Hall effect show a tendency for the number of carriers to decrease with increasing field. We thus find that the effective number of carriers at  $T = 0.5$  K and  $H = 200$  kOe, for example,<sup>70</sup> is  $7 \cdot 10^{18}$  holes/cm<sup>3</sup>. Near the threshold field, the data extracted on the number of carriers in this manner yield values ranging from 1% to 10% of the stoichiometric value. These results are not very accurate, and this interpretation of  $\rho_{xy}/H$  is probably ambiguous, since the field itself to some extent determines the mechanism for the formation of, and the parameters of, the new "semimetallic" phase. Nevertheless, we do take note of the fact that the Hall measurements near the threshold field yield a large "number of carriers." This fact seems to be related to yet another interesting result of Ref. 70: In very strong fields (10–20 T) and at rather high temperatures ( $T > 4$  K), the magnetoresistance of  $(\text{TMTSF})_2\text{ClO}_4$  exhibits classical Shubnikov–de Haas oscillations which are periodic along the  $1/H$  scale with a frequency  $\sim 275$  T. Such a frequency would correspond to a closed-orbit area amounting to 3.4% of the area of the Brillouin zone in the  $(a, b^*)$  plane.

In Fig. 17 the fields corresponding to the structural features in the Hall resistance at the various temperatures (shown by the points; the data are from Ref. 69) are shown together in the form of a phase diagram which depicts lines of transitions between various "subphases." (The other symbols in the region  $T \sim 1.5$ – $1.7$  K,  $H \sim 60$  kOe correspond to the observation of a boundary of a transition from the metallic phase to the magnetic phase according to calorimetric measurements,<sup>66,67</sup> NMR measurements,<sup>19</sup> and measurements based on the threshold field.) The points corresponding to the structural features in the Hall effect at  $T = 0.08$

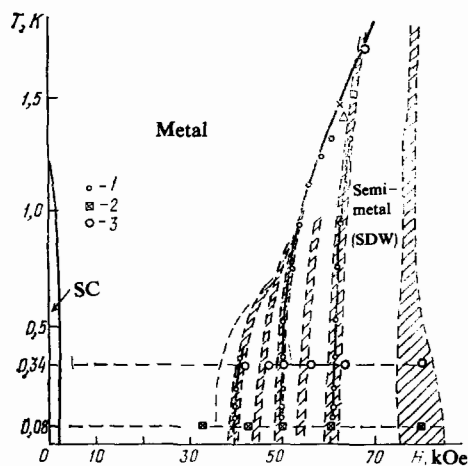


FIG. 17. Phase diagram of  $\text{ClO}_4$ . 1—A replotting of the data of Ref. 69 on the temperature dependence of the structural features in the Hall constant for  $\text{ClO}_4$  as a  $(T, H)$  phase diagram which exhibits several lines of transitions between different subphases; 2—structural features in the Hall effect observed in Ref. 70 (the hatched regions bounded by dashed lines show the temperature dependence of the fields of the "Shubnikov-de Haas oscillations"; the width of these regions is due to both the hysteresis in the phenomena and the imperfections in the reproduction of the results of Ref. 64 in this figure); 3—positions of the oscillation fields from Ref. 63. The symbols toward the upper right show earlier observations of a transition to a new phase found by a calorimetric method, by an NMR method, and from the threshold field.<sup>69</sup>

are taken from Ref. 70.

We stated above that the interpretation of the structural features in the Hall data as corresponding to a series of phase transitions which progressively reduce the number of carriers is only a guess. It nevertheless raises a question regarding the interpretation of the oscillations observed in the magnetoresistance (Fig. 12): Are these in fact Shubnikov-de Haas oscillations, or are the corresponding fields a "signature" of this series of hypothetical transitions? If the latter interpretation is correct, many of the unusual features of the temperature dependence and the shape of the signal and the temperature dependence of the oscillation frequencies themselves would become more understandable. Figure 17 shows the fields corresponding to the Shubnikov-de Haas oscillations for  $(\text{TMTSF})_2\text{ClO}_4$  according to the measurements in Ref. 63 at  $T = 0.34$  K. These fields offer some support for this guess. Kajimura *et al.*<sup>64</sup> measured the temperature dependence of the "oscillation" fields in the same compound and observed a hysteresis (which was particularly noticeable in strong fields) when the curves were plotted with decreasing field and with increasing field. In our opinion this hysteresis unambiguously resolves the question in favor of the existence of a series of transitions in a magnetic field. As for the agreement with the data of Refs. 63, 69, and 70 we note that the measurements in Ref. 64 were carried out—for some reason which is not clear to us—in a configuration in which the field  $H$  made an angle  $\theta \approx 33.5^\circ$  with the  $c^*$  axis. These results are shown in Fig. 17 after the appropriate conversion (a multiplication of the field values in Ref. 64 by  $\cos \theta = 0.84$ ) as the hatched bands, which reflect either the presence of hysteresis or, if this hysteresis is slight, the imperfection of our reproduction of the data of Ref. 64. The agreement is basically excellent. (The dashed line was found in Ref. 64 exclusively in measurements in an increasing field.) We note in conclusion that it is not clear at this point whether there is an important difference between the properties of  $(\text{TMTSF})_2\text{X}$  with  $\text{X} = \text{ClO}_4$  and  $\text{PF}_6$ . An experimental fact which has been established for  $\text{PF}_6$  is that the periodicity of the "magnetoresistance oscillations" along the  $1/H$  field is considerably better than that in  $\text{ClO}_4$ . It has been concluded<sup>70</sup> on this basis that the oscillations in Fig. 12 do in fact characterize the orbits of a new phase which arises above the threshold field. We have already mentioned the difficulty which stems from the circumstance that this is a second-order transition, so that it is not clear why the parameters of the new phase could be established in a field interval separating the threshold field from the field of the nearest oscillation. Furthermore, it was mentioned in Ref. 65 that in this case the areas of the orbits are not small, and this point is an argument in favor of a "direct" superposition vector (superstructure vector)  $(2k_F, 0, 0)$ . The differences in the anionic structure of the two compounds which we discussed above, while themselves small, could also influence these subtle phenomena.

## 8. THEORETICAL INTERPRETATION OF THE PHASE DIAGRAM

At this point we will not discuss why it is the antiferromagnetic phase, rather than a more common structural in-

stability, which occurs in the  $(\text{TMTSF})_2\text{X}$  compounds at low temperatures. We accept this result as an experimental fact. From the standpoint of the phase diagram in Fig. 4 we need to determine, first, the mechanism by which the spin ordering is suppressed by pressure (at  $H = 0$ ) and, second, why a spin density wave is then *restored* by a uniform magnetic field. These phenomena occur at such low temperatures ( $T_{\text{SDW}} \sim 10$  K and below) that we should seek some rather general microscopic mechanism.<sup>72</sup> The high-temperature "past history," i.e., the initial similarity between the structure of these compounds and a one-dimensional structure, may determine the choice between structural and magnetic instabilities, but in the subsequent phenomena this history will apparently not be as important. Estimates of the tunnel integrals,<sup>4,62,73</sup> which differ in some cases by a factor of two or three, nevertheless yield  $t_b \sim 100$ -200 K. Consequently, since the low-temperature state of the system exhibits a good metallic behavior it is natural to accept the standard theory of a Fermi liquid at the lowest temperatures and to assume that the electron spectrum in (3) is a spectrum of quasiparticles of an anisotropic metal with interactions. Either the tendency toward the formation of a spin density wave (Section 6) should be attributed to a gain in electron energy due to a good congruence during the superposition of the two open parts of the Fermi surface with  $\mathbf{Q} = (\pi/a, \pi/b^*, \pi/c^*)$  (Ref. 54), or the spin density wave should be regarded as a consequence of a 1D mechanism ( $g_3 \neq 0$ ; Section 2) which "survives" to low temperatures despite the significant values of the tunnel integrals in (3) (Ref. 23). In the latter case the value  $\mathbf{Q} = (\pi/a, 0, 0)$  could occur. For definiteness, we make this choice, on the basis of the preliminary indications in its favor which were discussed above.<sup>65,70</sup>

The tendency toward the formation of a spin density wave is expressed by a singularity in the generalized susceptibility  $\chi(\mathbf{Q})$ , which is the response of the electron spin subsystem to the weak "antiferromagnetic field of the sublattices":

$$\langle \hat{\sigma}(\mathbf{Q}) \rangle = \chi(\mathbf{Q}) \hat{\mathbf{h}}(\mathbf{Q}), \quad (6)$$

where

$$\hat{\mathbf{h}}(\mathbf{Q}) = h_0 \hat{\sigma}^{(y)} \exp(i\mathbf{Q}\mathbf{r}). \quad (7)$$

(Here the  $z$  axis runs parallel to the  $c^*$  axis, i.e., along the magnetic field; more-complicated helicoidal structures would be possible only in the incommensurable case.) This is the ordinary Overhauser mechanism: A modulation of the spin is caused by the pairing of an electron with one spin direction, near, say, the right-hand  $(+k_F)$  part of the Fermi surface, with a hole near  $-k_F$  for the branch of the spectrum with the opposite spin. [In a pairing of branches with identical spin projections in a charge density wave the nesting vector changes because of the additional separation of the Fermi surfaces corresponding to the different spin projections because of the term  $\mu_B(\partial H)$ .] The nesting mechanism causes an important gain in electron energy if the tendency toward pairing is great for electrons (holes) on the entire Fermi surface, i.e., when a pair with momenta  $\mathbf{p}$  and  $\mathbf{p} + \mathbf{Q}$  forms a coherent state which does not depend on the point  $\mathbf{p}_1$ . The equations for the wave functions of the elec-

trons on the right ( $+k_F$ ) and on the left ( $-k_F$ ) in the semiclassical limit are

$$\mp iv \left( \frac{d}{dx} \right) \tilde{\psi}_{p_{\perp}}^{\pm} + t_{\perp}(\mathbf{p}_{\perp}) \tilde{\psi}_{p_{\perp}}^{\pm} = (E - E_F) \tilde{\psi}_{p_{\perp}}^{\pm}, \quad (8)$$

where  $\tilde{\psi}_{p_{\perp}}(x)$  is the slowly varying part of the wave function [a factor of  $\exp(\pm ik_F x)$  has been extracted], and  $t_{\perp}(\mathbf{p}_{\perp})$  is the transverse dispersion of the electron spectrum. The term with  $t_{\perp}(\mathbf{p}_{\perp})$  in the solution of (8) for the wave functions of an electronhole pair ( $\psi_{\text{hole}} = \psi_{\text{electron}}^*$ ) contributes a phase factor which increases with  $x$ :

$$\exp \left[ \frac{i}{v} (t_{\perp}(\mathbf{p}_{\perp}) + t_{\perp}(\mathbf{p}_{\perp} + \mathbf{Q}_{\perp})) x \right]. \quad (9)$$

In the limit of complete nesting,  $t_{\perp}(\mathbf{p}_{\perp}) + t_{\perp}(\mathbf{p}_{\perp} + \mathbf{Q}_{\perp}) = 0$ , we denote the corresponding instability temperature by  $T_{\text{SDW}}^0$ . If this is not the case, the phase factor in (9) will disrupt the coherence of the state of the pair for different values of  $\mathbf{p}_{\perp}$ . With  $\delta t_{\perp} = t_{\perp}(\mathbf{p}_{\perp}) + t_{\perp}(\mathbf{p}_{\perp} + \mathbf{Q}_{\perp}) \neq 0$  the pairing is not disrupted immediately, however, as long as  $\delta t_{\perp}$  is still sufficiently small:  $\delta t_{\perp} \lesssim T_{\text{SDW}}^0$ . An increase in  $\delta t_{\perp}$  leads to a decrease in the temperature  $T_{\text{SDW}}$  ( $T_{\text{CDW}}$ ) and ultimately a restoration of the metallic state. Let us assume that the role of the pressure is one of changing  $\delta t_{\perp}$  (Ref. 74). With respect to spectrum (3) and the vector  $\mathbf{Q} = (2k_F, 0, 0)$ , this assumption means that  $t_b$  would increase with the pressure and reach a critical value  $t_b^*$  at  $P = P_{\text{cr}}$  (Fig. 4).

We assume  $P > P_{\text{cr}}$ , and we assume that the state at  $T = 0$  corresponds to a metallic phase. We introduce a magnetic field in (8) through the customary substitution  $\mathbf{p} \rightarrow \mathbf{p} - (e/c)\mathbf{A}$ . Taking the geometry  $(\mathbf{H}) \parallel c^*$  into account, we choose  $\mathbf{A} = (0, Hx, 0)$ . In (8) we now have

$$\mp iv \left( \frac{d}{dx} \right) \tilde{\psi}_{p_{\perp}}^{\pm} + t_{\perp} \left( \mathbf{p}_b - \frac{e}{c} Hx, \mathbf{p}_c \right) \tilde{\psi}_{p_{\perp}}^{\pm} = (E - E_F) \tilde{\psi}_{p_{\perp}}^{\pm}.$$

The solution for the wave function is

$$\tilde{\psi}_{p_{\perp}}^{\pm}(x) = \exp \left[ \pm \frac{i}{v} (E - E_F) x \right] \mp \frac{i}{v} \int dx' t_{\perp} \left( \mathbf{p}_b - \frac{e}{c} Hx', \mathbf{p}_c \right) \tilde{\psi}_{p_{\perp}}^{\pm}.$$

It follows rigorously from this result for a *two-dimensional* (layered) structure that, in contrast with (9), the phase factor of the wave function of the pair in a field is necessarily bounded:

$$\exp \left\{ \frac{i}{v} \left[ \tilde{t} \left( \mathbf{p}_b - \frac{e}{c} Hx \right) + \tilde{t} \left( \mathbf{p}_b + \mathbf{Q} - \frac{e}{c} Hx \right) \right] \right\}. \quad (9')$$

Specifically,

$$\tilde{t}(x) = \int dx' t_{\perp} \left( \mathbf{p}_b - \frac{e}{c} Hx' \right) \sim \frac{c}{eH} t_{\perp}$$

is a periodic function, as is clear from the conservation of the number of electrons in a cell. The physical meaning of this result is that an electron and a hole with longitudinal momenta  $\pm k_F$ , moving at identical velocities  $v$  along the  $x$  axis, do not go off to infinity in the transverse direction: In a magnetic field, the effects of the crystal lattice [the periodicity of  $t_{\perp}(\mathbf{p}_{\perp})$ ] keep the transverse motion of the particles fin-

ite. (This effect is semiclassical: The electron trajectories are open!) The magnetic field "one-dimensionalizes" the motion of the electrons.

A 2D system is thus always unstable with respect to a pairing of the nature of a spin density wave in an arbitrarily weak field (if the interactions have the appropriate sign; the effect of the field on a charge density wave will be discussed below). In the  $(\text{TMTSF})_2\text{X}$  salts, the anisotropy along the  $c$  axis is pronounced ( $t_c/t_b \sim 1/10-1.30$ ). In the case of a "direct" nesting vector, the transition from the phase of the spin density wave to the metallic phase is attained through an increase in  $t_b > t_b^*$ . In the 2D case, however, the metallic phase would be unstable in an arbitrarily weak field, but the finite value of  $t_c$  means that the instability would occur only above a certain threshold field.

This effect is incorporated in the behavior of the generalized susceptibility  $\chi(\mathbf{Q})$  of the metallic phase (at  $t_b > t_b^*$ ). For a calculation we use the standard expression

$$\chi(\mathbf{Q}) = \chi_0(\mathbf{Q}) [1 - \lambda \chi_0(\mathbf{Q})]^{-1}, \quad (10)$$

where  $\chi_0(\mathbf{Q})$  is the response of the noninteracting electrons to the field in (7), and  $\lambda$  is an appropriate interaction constant (see Ref. 53, for example). If the metallic phase is to be stable, the denominator in (10) must be positive.

These ideas cannot be refined further without making use of a specific dispersion  $t_{\perp}(\mathbf{p}_{\perp})$ . For the  $(\text{TMTSF})_2\text{X}$  compounds, with only one filament per unit cell, expression (3) is an extremely plausible expression for the shape of the spectrum. We wish to emphasize this reservation, since the choice of spectrum (3) leads to some results which pertain to only this special dispersion law [for example, there would not be an exact superposition of the branches for the superstructure vector  $(2k_F, \pi/b^*, \pi/c^*)$  for just any arbitrary dispersion law]. Some of these results have some direct experimental consequences.

Taking  $t_{\perp}(\mathbf{p}_{\perp})$  from (3), we can put the condition for stability of the metallic phase in the following form<sup>72</sup>:

$$\xi^{-1} - \int_d^{\infty} J_0 \left( \frac{8ct_b}{veHb^*} \sin \frac{eHb^*x}{2c} \right) J_0 \left( \frac{4tcx}{v} \right) \cdot \frac{2\pi T \cos kx dx}{v \text{sh}(2\pi T x/v)} \geq 0; \quad (11)$$

here  $\xi^{-1} = \lambda b^* c^* / 2\pi v$  is a dimensionless interaction constant, and  $d$  is the parameter of the logarithmic cutoff at small  $x$ :  $\xi^{-1} = \ln(v/\pi T_{\text{SDW}}^0 d)$ . The factor  $\cos kx$  arises in (11) because we will be concerned below with the stability of the metallic phase with respect to wave vectors

$$\mathbf{Q} = (2k_F + k, 0, 0). \quad (12)$$

The special role played by the magnetic field can be seen in the circumstance that the first of the Bessel functions in integral (11) does not lead to a cutoff at large  $x$ . Consequently, at  $t_c = 0$  ( $t_c \ll t_b$ ; the 2D situation) the integral over  $x$  diverges logarithmically not only at small  $x$  but also as  $x \rightarrow \infty$ , where only the temperature factor is responsible for a cutoff. Using the familiar expression (the theorem for combining Bessel functions)

$$J_0(2\lambda \sin \varphi) = J_0^2(\lambda) + 2 \sum_{n=1}^{\infty} J_n^2(\lambda) \cos 2n\varphi$$

using the condition for the stability of the metallic phase which is found from (11) in the case  $H \equiv 0$ , and assuming the temperature to be low, we find, with logarithmic accuracy,

$$\ln \frac{t_i}{t_b^*} = J_n^2(\lambda) \ln \left( \frac{\hbar v n}{2\pi T x_H} \right), \quad (13)$$

where

$$\lambda = \frac{4ct_b}{veHb^*}, \quad x_H = \frac{2c\hbar}{eHb^*}, \quad k = n \frac{eHb^*}{c} \quad (14)$$

(the lower cutoff at  $x_H/n$  is, strictly speaking, valid at sufficiently large values of  $n$ ). At  $t_c \neq 0$ , there is also a cutoff at large  $x$  in (11) because of the second Bessel function. Replacing  $\hbar v/2\pi T$  by  $\hbar v/4t_c$  in (13), we find an expression for the threshold field at  $T = 0$ . At nonzero temperatures and with  $t_c \neq 0$ , numerical methods must be used to study condition (11), but no such study has so far been carried out. We can, however, draw some conclusions from the results given above.

1) The value of  $\lambda$  is evidently large. The coefficients  $J_n^2(\lambda)$  in (14) are correspondingly small. Their small value may be offset to a large extent by the small value of  $\ln(t_b/t_b^*)$ , which means proximity to the boundary for the transition from the metallic phase to the antiferromagnetic phase. In other words, the magnetic field becomes increasingly important near  $P_{cr}$ .

2) In the case of a charge density wave the orbital effect competes with the spin effect. Because of the spin effect, the Fermi surfaces for electrons with opposite spin orientations have different superposition vectors,  $2k_F \pm 2\mu_B H/v$ . The choice of one of these vectors (in the 1D limit!) would mean that only half the number of electrons which are responsible for the structural transition at  $H = 0$  participate in the pairing; i.e., the transition temperature decreases. (In the 1D model a soliton phase forms at intermediate fields.<sup>75</sup>) It is the strong-field limit ( $\lambda \rightarrow 0$ ) which corresponds to the 1D problem, according to (11). In this limit the pairing of the spin density wave is intensified, while the charge density wave gradually breaks up. At a finite value of  $t_1$  we need to compare the energy  $\mu_B H$  with  $t_1$ , and we again find a dimensionless order parameter  $\lambda$ . Accordingly, for a charge density wave near the threshold (in the pressure) the two mechanisms by which the magnetic field acts work opposing each other. Their contribution depends on the particular choice of transverse dispersion  $t_1(\mathbf{p}_1)$ . If this dispersion is similar to that in (3), the spin mechanism will not be important in moderate fields.

3) Expression (13) for  $T_{SDW}$  (or for the threshold field) of the spin phase induced by a magnetic field holds specifically for the simple dispersion law in (3) (at  $t_c \ll t_b$ ). A distinctive feature of the 2D dispersion model (3) from the mathematical standpoint is that it is degenerate in the absence of a field.<sup>76</sup> Traces of this degeneracy can be seen in (13): At  $n \sim 1$  and  $\lambda \gg 1$  the asymptotic behavior

$$J_n^2(\lambda) \approx \frac{2}{\pi\lambda} \sin^2 \left( \lambda - \frac{\pi}{4} \right)$$

is the same for all  $k$  from (14) for  $k \ll 4t_b/v$ . The greatest value at  $\lambda \gg 1$ , however, is that of  $J_n(\lambda)$  with  $n \approx \lambda$ :

$$J_n(\lambda) \approx \frac{\sqrt{2}}{\Gamma(2/3) 3^{2/3} \lambda^{1/3}}.$$

We thus see that near the critical temperature (or the threshold field) Eq. (13) selects a structure of the spin density wave with a wave vector  $\mathbf{Q}$  near  $(2k_F + 4t_b/v, 0, 0)$ . The exact value of the wave vector (and of the transition temperature) oscillates with the magnetic field ( $n$  is the greatest integer below  $\lambda$ ) with a period

$$\Delta \frac{1}{H} = \frac{eb^*v}{4ct_b}. \quad (15)$$

The "area of the orbits," i.e., of the pockets, which result from the superposition of the two parts of the Fermi surface with the vector  $(2k_F + 4t_b/v, 0, 0)$  is (Fig. 18)

$$S = \frac{8t_b\pi}{\hbar v b^*}. \quad (16)$$

Expression (15) then becomes

$$\Delta \frac{1}{H} = \frac{2\pi e\hbar}{cS}. \quad (17)$$

These expressions are consistent with two experimental results: the large number of carriers ( $\sim 10^{20} \text{ cm}^{-3}$ ) near the threshold field at low temperatures, as determined from the Hall effect,<sup>69,70</sup> and the high oscillation frequencies of the magnetoresistance in strong fields and at high temperatures, which correspond to<sup>70</sup>  $S \approx 3.4\%$  of  $S_{ZB}$ . Assuming  $v = t_a a/\sqrt{2}\hbar$ , as is customary in the literature ( $t_a$  is the tunnel integral along the chain), we find  $S = (2\sqrt{2}t_b/\pi t_a) S_{ZB}$  from (17) and thus  $t_b/t_a \sim 1/27$ . This is not an unsatisfactory result in view of the approximate nature of the estimates of the anisotropy of  $t_b$  and  $t_a$  from the anisotropy of the conductivities. An estimate from (17), however, would exaggerate the frequencies of the "Shubnikov oscillations" (the fields of the series of phase transitions) by a factor of two or three in the case of  $\text{PF}_6$  (Ref. 17). It can be assumed that at low temperatures the superposition vector is near  $(2k_F, \pi/b^*, \pi/c^*)$ . The results above can also be generalized quite easily to this case, under the assumption  $t_1(\mathbf{p}_1) = t_1^{(0)}(\mathbf{p}_1) + t_1'(\mathbf{p}_1)$ , where  $t_1^{(0)}(\mathbf{p}_1)$  is again given by (3) but does not drop out of Eqs. (9) and (9') for this choice of the vector  $\mathbf{Q}$ , while  $t_1'(\mathbf{p}_1)$  is responsible for the violation of the

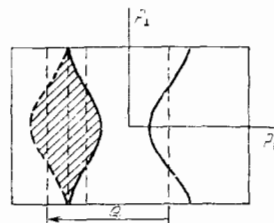


FIG. 18. Cosinusoidal curves about the dashed lines at  $\pm k_F$ : the shape of the Fermi surface according to (3). The superposition vector  $\mathbf{Q} = (2k_F + 4t_b/v, 0, 0)$ , predicted theoretically,<sup>72</sup> corresponds to the formation of large electron (or hole) pockets (the hatched region).

condition for the ideal superposition of the two parts of the Fermi surfaces. It has already been shown,<sup>65</sup> however, that  $t'_1(\mathbf{p}_1)$  is probably too small to explain the orbit areas found. It is our opinion that the superstructure vector near the transition temperature does not determine the ground state at low temperatures. The energy of this state and its symmetry must be determined through a solution of the complete problem, in which the energy spectrum and the structure of the new magnetic phases must be sought, generally speaking, in the presence of a quantizing magnetic field. Until these calculations are carried out, the question will remain open.

We do not yet have any experimental data which reveal the temperature of the transition from the metallic phase to the antiferromagnetic phase at  $T > 4$  K. The NMR method detects the magnetic moment of the sublattices of a new phase only if this moment is quite large. For this reason, the oscillations of the magnetoresistance observed in Ref. 70 in strong fields and at high temperatures (up to 10 K) can be attributed to both oscillations of the wave vector of the phase of the spin density wave with the field, in accordance with (15), and oscillations of the same nature but in the mechanism for the relaxation of the metallic phase: The electron-electron scattering, which is probably responsible for the resistance at low temperatures, includes a channel corresponding to scattering by virtual "spin waves"—paramagnons. Above the transition temperature, this mechanism strengthens with decreasing value of the denominator in (10); i.e., the fluctuations increase as the system approaches the transition to the phase of the field-induced spin density wave.

## 9. THE FLUCTUATION PROBLEM

One of the most interesting questions which has been raised in connection with the many nontrivial properties of these new materials is that of the role played by so-called superconducting fluctuations or, in a broader sense, the importance of 1D effects. At high temperatures the transverse dispersion of the electron spectrum of course plays no fundamental role if  $2\pi T > 2t_b$ . The transition region is therefore characterized by a scale temperature  $T^* \sim t_b/\pi \sim 70\text{--}50$  K. The question is therefore one of whether the 1D instability mechanisms discussed in introductory Section 3 are able to impose a scale energy comparable to  $T^*$  on the system. The French group at Orsay answers this question in the affirmative,<sup>4,77-79</sup> thereby asserting that the  $(\text{TMTSF})_2\text{X}$  compounds constitute the first example of materials in which the superconductivity mechanism differs from the phonon mechanism of the Bardeen-Cooper-Schrieffer theory. Their arguments run as follows.

In these compounds, there is no Peierls (structural) instability. A theoretical condition for the suppression of this instability by electron-electron interactions (Section 2) is the relation between the interaction constants,  $2g_2 - g_1 < 0$  ( $g_1 > 2g_2 + |g_3|$ ) when spin flip is taken into account). If the condition  $g_1 > 0$  also holds (a Coulomb repulsion), then there will be a mutual rescreening of the electron-electron interactions according to (2), with the result that we would have

$$\tilde{g}_1 \approx 0, \quad \tilde{g}_2 = g_2 - \frac{1}{2}g_1 < 0. \quad (18)$$

In other words, the effective amplitude of the back-scattering is small, and the scattering with a small momentum transfer (forward scattering) has an attractive sign (despite the fact that all the interactions are of a Coulomb nature!). This attraction is seen in the tendency toward Cooper pairing (this pairing could be either a singlet or triplet pairing; another possibility in the 1D model, with an adequate value of  $g_3$ , would be the formation of a commensurate spin density wave). The temperatures to which (2) and (18) apply are  $T_{\text{MF}} \sim E_{\text{F}} \exp(-1/g_1)$ .

At  $T < T_{\text{MF}}$ , a "superconducting gap" develops, but there is no long-range order, and the "superconductivity" exists in regions with dimensions of the order of the correlation lengths. The 3D effects ultimately establish a long-range order. These representations are of course noncontradictory at a qualitative level if  $T_{\text{MF}} \gtrsim T^*$ . Unfortunately, a rigorous theoretical solution of the problem cannot be found. The theoretical work which has been carried out (and which is reviewed in Refs. 4 and 78) has been aimed at a quantitative description of the experimental data in a phenomenological model of nonlinear fluctuations, and the desired goal—a superconducting gap—is embodied in the model at the very beginning. The agreement with experiment which is reached with an appropriate choice of parameters is still not proof, and we will discuss the available set of experimental data at a qualitative level below, comparing this hypothesis with both the experimental information itself and the possibility of alternative explanations.

A few words are in order regarding the 3D superconductivity in these compounds. This superconductivity is observed at  $T_c \sim 1$  K (either under pressure, as in  $\text{PF}_6$ , or at  $P = 0$ , as in  $\text{ClO}_4$ ). Figure 19 is a typical phase diagram. The superconducting phase has now been studied quite thoroughly, and in general it can be described by the ordinary microscopic BCS theory for an anisotropic metal. Even the increased sensitivity of  $T_c$  to defects can be understood if one assumes that the defects in compounds of this type apparently correspond to localized spins and serve as paramagnetic centers (see the review by Buzdin and Bulaevskii for a discussion of the properties of the superconducting phase). The only point which would raise any eyebrows would be the rapid decrease in  $T_c$  with the pressure: Since the superconducting phase borders the magnetic phase of the spin density

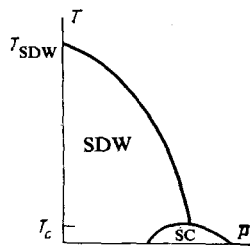


FIG. 19.  $(T, P)$  phase diagram which shows schematically the relative behavior of the phase of the spin density wave and of the superconducting phase with the pressure.



wave, we cannot rule out a possible role of spin fluctuations (paramagnons).

The basic arguments in favor of a fluctuational superconductivity come from the list of anomalous or, more precisely, unusual properties of these compounds at a higher temperature (above  $T_c$ ) in the metallic phase. Here are these facts:

1. The huge conductivity (the values of  $\sigma$  range up to  $10^6$  S/cm) at liquid-helium temperatures. No residual resistance is observed down to the very lowest temperatures. If this fact is attributed to the high quality of the crystals, then the increase in the conductivity would occur against the background of a decrease in the state density at the Fermi level with decreasing temperature (we will return to this point below).

2. The large positive longitudinal magnetoresistance  $\Delta\rho(H)/\rho_0 \sim 1$  in weak fields ( $H < 20$  kOe), with an open Fermi surface. In turn, the magnetoresistance depends on the temperature down to the very lowest temperatures.

3. The fact that spin-flip processes due to electron-electron collisions,  $\tau_{ee}^{-1} \propto T^2/t_b$ , would be the predominant kinetic mechanism at low temperatures in the absence of impurities and collective effects. The effect of a weak magnetic field (below the threshold field  $H_0$ ) on the relaxation rate (the magnetoresistance and the magneto-thermo-emf<sup>62</sup>) would also be difficult to explain in terms of the phenomena which were proposed above in an effort to explain the nature of the phases of the spin density wave at  $H > H_0$ .

4. The semiphenomenological Kohler's rule, according to which  $\Delta\rho(G)/\rho_0$  is a function of  $H/\rho_0$  alone if a common kinetic mechanism is responsible for the magnetoresistance and for the resistance itself. This law does not hold [in (TMTSF)<sub>2</sub>ClO<sub>4</sub>; Refs. 80 and 81] at  $T \lesssim 30$  K.

5. The anomaly in the thermal conductivity at the same temperatures for both ClO<sub>4</sub> and PF<sub>6</sub> (under pressure).<sup>82,83</sup> On the one hand, the thermal conductivity appears to be due to electrons, as is implied by the fact that the Wiedemann-Franz law holds at high temperatures and the fact that there is no maximum in the thermal conductivity associated with the "freezing out" of phonon spin-flipping processes (as would be the case for a lattice contribution). The thermal conductivity decreases (the electrical conductivity increases) at  $T < 25$  K, but this decrease can be offset by a magnetic field. This fact is regarded as proving that the anomaly in the thermal conductivity is electronic in nature. On the contrary, this result appears to be the first piece of evidence that the anomaly is of a different nature: At low temperatures the magnetic field which restores the value of the thermal conductivity is unexpectedly low (2–3 kOe) and exceedingly close to the field values at which spin flipping occurs in the antiferromagnetic phase of the spin density wave at  $P = 0$ .

6. The two components, phonon and electronic, of the specific heat of ClO<sub>4</sub> at low temperatures<sup>66</sup>:

$$C(T) = \gamma T + \beta T^3.$$

The high magnetoresistance in comparatively weak fields and several other features are in accordance with a strong field dependence of the coefficient  $\gamma$  in the electron component of the specific heat.<sup>67</sup> The coefficient  $\gamma(H)$  itself

increases with increasing field at a given temperature.

The effect is strong even in fields  $H \lesssim 20$  kOe, at which we have  $H < H_0$ . The value of  $\gamma(H)$  is customarily understood as a measure of the state density at the Fermi level,  $\nu(E_F)$ . These valuable results thus require a second look at what we know about the structure of the state density near the Fermi level.

## 10. STRUCTURE IN THE STATE DENSITY

This structure in ordinary superconductors is studied in metal-insulator-superconductor tunnel contacts. In (TMTSF)<sub>2</sub>PF<sub>6</sub> superconductivity and the metallic state exist under pressure at low temperatures; accordingly, the tunnel barrier used in Refs. 62 and 63 was a Schottky barrier at the interface between (TMTSF)<sub>2</sub>X and a sputtered film of a semiconductor, *n*-type GaSb (the results are described in Ref. 4). Figure 20 sketches the basic idea of these experiments: The quantity  $R_{\max}$ , i.e., the resistance of the barrier with a small potential difference  $V$ , is proportional to the state density at the Fermi level. In a superconductor this state density increases with the field and with increasing temperature. This is the behavior which was observed in Refs. 62 and 63; the temperature interval over which there was a marked change in  $R_{\max}$  was estimated to be about 10–15 K. The field dependence of  $R_{\max}$  (a "field-induced disruption of superconductivity") was followed up to  $H \sim 30$  kOe. The peak in the resistance (at  $V = 0$ ) was also found in the case in which there was a gap of insulator origin in the spectrum. The dependence on the magnetic field is thus a fundamental result and is interpreted as a magnetic-field induced disruption of a superconducting "pseudogap." The pseudogap  $2\Delta$  itself is determined by the procedure illustrated in Fig. 20. In the BCS theory the dip in the state density at  $\epsilon > \Delta$  gives way to a square-root singularity at  $\epsilon = \Delta$ , which leads to minima in the resistance at  $eV = \Delta$ . The pseudogap determined in this manner is about 3–3.6 meV. Similar results have been found<sup>85,86</sup> for (TMTSF)<sub>2</sub>ClO<sub>4</sub>. Interestingly, the same tunnel measurements reveal structural features on the voltage-current characteristic at the lowest temperatures which stem from an ordinary (3D) low-temperature superconductivity; the size of the superconducting gap and the transition temperature are related by the relation of the BCS theory.

In evaluating these results we note that they are evidence of structure in the state density with a typical size of 3–4 meV (a pseudogap). The conclusion that this pseudogap is of a superconducting nature is again based on the magnetic-

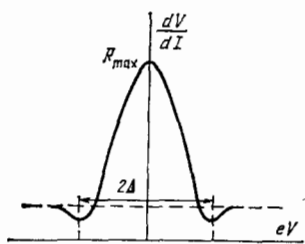


FIG. 20. Typical curve of the resistance of a tunnel contact as a function of the applied potential difference  $V$ .

field dependence of the tunnel characteristics [more precisely, on  $R_{\max}(H)$ ].

The classical method for observing a superconducting gap is to measure the absorption of infrared light: The quantity  $2\Delta$  is the threshold above which a photon with  $\hbar\omega > 2\Delta$  can be absorbed. In the experiments of Ref. 87 a threshold was observed [for  $(\text{TMTSF})_2\text{ClO}_4$ ], and the data on the pseudogap agree well with the results of the tunnel experiments. Furthermore, a field dependence of the absorption was reported in Ref. 87.

The results which we have reviewed up to this point on the structure of the state density reproduce the basic properties which would be exhibited by a superconductor with a gap  $2\Delta$  of about 30–50 K. Some new features were observed in some recent studies,<sup>88,89</sup> where a more detailed study was made of both the magnetoabsorption and the reflection coefficient of polarized light. Careful measurements of this reflection carried out over a broad frequency range, with subsequent processing of the results by the Kramers-Kronig relations, made it possible to construct the frequency dependence of the longitudinal conductivity,  $\sigma(\omega)$ .

In Refs. 88 and 89 the reflection coefficient for  $(\text{TMTSF})_2\text{ClO}_4$  was measured to about 2 K over the frequency range from 5 to 400  $\text{cm}^{-1}$  and from 4 to 40  $\text{cm}^{-1}$ , respectively. In order to analyze the data by means of the Kramers-Kronig transformation it is necessary to join these results with the high-frequency results reported by other investigators (the results of these two studies agreed). The reflection coefficient is observed to decrease at two frequencies:  $\sim 7 \text{ cm}^{-1}$  and  $\sim 30 \text{ cm}^{-1}$ . Structural features in the absorption are observed at the same frequencies. So far, it has been difficult to interpret the first peak in the conductivity; it is sensitive to a weak magnetic field.<sup>89</sup> The second peak, at  $\sim 30 \text{ cm}^{-1}$ , should be identified with the size of the pseudogap. The second peak, however, is also seen at higher temperatures (up to 60 K); as the temperature is raised, this peak shifts essentially instantaneously from 29  $\text{cm}^{-1}$  to 25  $\text{cm}^{-1}$  at temperatures near the anionic-ordering temperature, 24 K. The corresponding frequency seems to be related in some way to the energy required to overcome an activation barrier for an orientational transition, and this energy is acquired from conduction electrons in the course of their interaction with anions. This peak is also sensitive to only a weak magnetic field: The dependence on the magnetic field reaches saturation at  $H \sim 2 \text{ kG}$ . These fields and temperatures are very close to those characterizing the structural feature in the behavior of the thermal conductivity. At any rate, we get the impression that the two phenomena are related, although we do not have a clear physical explanation. These results will undoubtedly require a second look at the interpretation of Ref. 87, where this frequency was identified with the size of the superconducting pseudogap. It will probably also be necessary to take a second look at the tunnel data of Ref. 86. Consequently, at least for  $(\text{TMTSF})_2\text{ClO}_4$ , we do not yet have any incontrovertible evidence for a well-developed superconducting pseudogap; the structural features in the conductivity observed at these frequencies are more likely to stem from an anionic ordering. The particular magnetic

fields which are of importance here probably indicate interactions of a magnetic-anisotropy type.

The measurements in Refs. 90 and 91 were carried out over a broad frequency range but correspond to higher temperatures (above 25 K). For  $(\text{TMTSF})_2\text{PF}_6$  the frequency dependence of the longitudinal conductivity (at 25 K) exhibits a virtual gap at 180  $\text{cm}^{-1}$ . This "gap" is considerably larger than that which would follow from the results of the tunnel measurements,<sup>84,85</sup> and it is observed above the temperature of the ordering of the antiferromagnetic phase. This frequency apparently cannot yet be identified with any phonon mode excited by conduction electrons.<sup>91</sup> In the light of the results on  $(\text{TMTSF})_2\text{ClO}_4$ , for which the pseudogap frequency found from the tunnel data is related to an anionic-ordering transition, it is pertinent to recall what was stated in Section 5 regarding the data of Refs. 39 and 40 on the asymmetry of the octahedral anions. The values found for  $2\Delta$  for  $\text{ClO}_4$  and  $\text{PF}_6$  (under pressure) are in approximate agreement<sup>84,85</sup> and, in the case of  $\text{PF}_6$ , may also characterize an analogous degree of freedom, especially since the latter compound exhibits an anomaly in its thermal conductivity.

## 11. INTERPRETATION OF THE OBSERVED STRUCTURE

In summary, for  $(\text{TMTSF})_2\text{ClO}_4$ , at least, the "structure" in the state density is probably not due to a superconducting "pseudogap." At  $2\Delta \sim 3\text{--}4 \text{ meV}$ , a structure is observed in the infrared spectrum up to 60 K. The frequency position itself changes only slightly, and this change occurs at the anionic-ordering temperature. As yet we do not have an explanation for these features. They are undoubtedly related to the anomalies in the behavior of the thermal conductivity in the same temperature range. As for the anionic ordering with the vector  $(0, \pi/b, 0)$ , it should correspond to additional structure in the state density (probably a small structure) due to the formation of "gaps" at the boundary of a new band. We must await corresponding optical measurements, which would make it possible to find quantitative results on the corresponding changes in the electron spectrum.

The question of a "pseudogap" could be raised equally well in connection with a spin density wave, which arises in the 1D model if  $g_3 \neq 0$  (Ref. 9; see Section 2 of the present paper). Furthermore, a rigorous solution of Hubbard's 1D model in the case of precisely one electron per cell corresponds at  $T = 0$  to a ground state with an antiferromagnetic gap.<sup>92,93</sup> If this solution is to be pertinent, the gap  $\Delta$  must be comparable to or greater than  $T^*$ . The only fact which can be discussed on this basis is the optical gap ( $\sim 180 \text{ cm}^{-1}$ ) in  $\text{PF}_6$  at  $T = 25 \text{ K}$  (above  $T_{\text{SDW}}$ ).<sup>91</sup> There is no degree of freedom associated with the shift of the spin density wave in the commensurate case, and the fluctuations of the size of the pseudogap are small at low temperatures. We are left with the problem of matching the directions of the sublattice of spins on adjacent filaments. In the model of Section 2 this function (the function of an exchange between chains) is performed by a transverse dispersion of the electron spectrum which results from a transverse overlap of the wave functions of the electrons.

We have repeatedly stressed that, because of the particular properties of spectrum (3), a 3D ordering mechanism of this sort would probably lead to a superstructure “superposition” vector  $\mathbf{Q} = (\pi/a, \pi/b)$ , while magnetotransport phenomena (Sections 7 and 8) imply a vector  $\mathbf{Q} = (\pi/a, 0)$  (or a vector representing an intermediate case between the two<sup>65</sup>).

There is, however, yet another possibility for a 3D ordering of a spin density wave. A 3D transition to an antiferromagnetic phase and the structure vector of this phase can be fixed<sup>12</sup> (even if  $g_3, t_1 = 0$ ) if we assume that spin (exchange) forces as well as Coulomb forces act between different chains. We will not take up the origin of these spin forces, which might be “indirect exchange” forces, etc., resulting from some structure in the conducting system of Se–Se contacts<sup>94</sup> more complicated than that of the model of Refs. 8 and 9. Symmetry considerations make it likely that  $\mathbf{Q}_1$  would either be zero or lie at a zone boundary. In the latter case, we would again be unable to distinguish this mechanism from the effects of a superposition. If  $\mathbf{Q} = (\pi/a, 0)$ , however, then the electron dispersion in (3) would clearly hinder an antiferromagnetic ordering, and this ordering would occur in contradiction of (4). A nonzero value of  $t_b$  reduces  $T_{\text{SDW}}$  (from the value of  $T_{\text{SDW}}^0$  at  $t_b \equiv 0$ ). If  $t_b > t_b^*$ , where the right side is the corresponding critical value ( $P > P_{\text{cr}}$ ), then the metallic phase would stabilize.<sup>3)</sup>

We assume  $t_b \neq 0$  but  $t_b < t_b^*$ . We note that the “gap” (more precisely, the order parameter  $\Delta$ ) at low temperatures is not related to  $T_{\text{SDW}}$  by the BCS relation. The electron spectrum in this case is

$$\varepsilon(\mathbf{p}) = 2t_b \cos pb^* + 2t_c \cos \widehat{pc}^* \pm \sqrt{\xi^2 + \Delta^2}. \quad (19)$$

As long as the condition  $2(t_b + t_c) < \Delta$  holds there will be no pockets, and  $\Delta$  at  $T = 0$  will be completely independent of  $t_b$  (Ref. 74). In particular,  $T_{\text{SDW}}$  can be low ( $T_{\text{SDW}} \ll T_{\text{SDW}}^0$ ), while  $\Delta(0)$  is still large (in the simple model of Section 8 we would have  $\Delta(0) \approx \pi/\gamma T_{\text{SDW}}^0$ ). It can be seen from Fig. 21 that at low temperatures spectrum (19) has two gaps: an indirect or activation gap  $2(\Delta - 2t_b)$ , responsible for the number of carriers at  $T \ll \Delta$ , and a direct gap  $2\Delta$ , which is pertinent to the optical absorption. If the pockets overlap slightly, there will be no activation gap at all. With increasing temperature, the order parameter is rapidly disrupted by the thermal filling and expansion of the pockets. We know that in the phase of the spin density wave in  $\text{PF}_6$  the conductivity remains semimetallic in the limit<sup>52</sup>  $T \rightarrow 0$ , while in  $\text{AsF}_6$  the activation gap is about<sup>21</sup> 25 K. The values of  $T_{\text{SDW}}$  in the two compounds are approximately the same. If we assume that the data of Ref. 91 characterize the direct gap in  $\text{PF}_6$ , then we need to recall that these results were obtained at  $T > T_{\text{SDW}}$ . It is not clear whether we can speak in terms of a well-developed gap above the 3D-ordering temperature.

Indeed, it might appear that similar questions related to a pseudogap should arise in corresponding cases with an in-

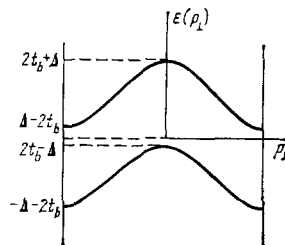


FIG. 21. The spectrum in (19) as a function of the transverse momentum. This spectrum has a direct optical gap of  $2\Delta$  and an indirect (activation) gap of  $2\Delta - 4t_b$ .

ulating transition of the Peierls type. This is the point of view in the review by Jerome and Schulz,<sup>4</sup> for example. In our opinion, however, there is always a simpler way to describe the basic results. During a structural transition at high temperatures, diffuse lines are observed: 1D “presursors” of a 3D Kohn anomaly. With decreasing temperature, these lines gradually acquire a 3D nature. The 3D phase transition ultimately completes the conversion to the new phase. All this fits qualitatively into the picture of the role played by the 3D effects<sup>11</sup> mentioned in Section 2. Over a rather broad temperature range near  $T_p$  we can speak in terms of fluctuations, but in the ordinary sense—that the phase transition does not conform very well to Landau’s phenomenological theory. In our opinion there is no special reason to believe that a structural parameter or the amplitude of the charge density wave will already have formed on each filament by the time of the transition or that there will be no long-range order because of fluctuations in its phase. Critical scattering near the point of the 3D transition would not make any great contribution to the resistance. Those features which are sometimes attributed to a fluctuational contribution from a Fröhlich mode<sup>4</sup> can also be explained on the basis of other effects, e.g., a phonon drag.<sup>94,96</sup> We expect a similar situation in the case of a spin density wave: Although in this case we do not have a convenient method such as x-ray structural measurements for monitoring the onset of an instability, there is also no direct evidence for a Hubbard gap.<sup>9,92,93</sup> The results of Ref. 91 can probably be explained in terms of an interaction of conduction electrons with the lattice (anions). The resistance does not exhibit a regime of strong critical fluctuations near  $T_{\text{SDW}}$  (Ref. 1). The model with the Overhauser mechanism (Section 8) can probably be used qualitatively over the entire temperature range  $T \sim T_{\text{SDW}}$ . This mechanism is capable of generating quantitative results only at low temperatures, where the behavior of the electrons conforms to the theory of a Fermi liquid.

The temperatures at which these ideas apply, and the extent to which they apply, are determined by fluctuations or, more definitely, spin fluctuations. In speaking of spin fluctuations we mean phenomena analogous to the fluctuations and “paraconductivity” phenomena in the theory of superconductivity.<sup>97</sup> Their contribution to the BCS theory is small if the ratio  $T_c/E_F$  is small. In the case of Q1D conductors (in this case we are considering the fluctuations associated with a spin-density-wave transition), the corresponding parameter would either be  $T_{\text{SDW}}/t_1$  or be determined by the

<sup>3)</sup>The second structure vector can be eliminated by assuming that the interaction constant which corresponds to it has the wrong sign for the formation of a spin density wave. A rigorous determination of the structure vector would require a solution of the “fast-parquet” equations.<sup>11,12</sup>

dispersion of the interaction constants and would be small only if these interactions were weak.<sup>11</sup> In other words, the interaction of electrons with the spin channel—paramagnons—is not weak (in the mechanism described above for the formation of the antiferromagnetic phase) and might play a nontrivial role, primarily for the superconductivity.

In Section 9 we listed the arguments of the Orsay group in favor of a nontrivial superconductivity mechanism in the (TMTSF)<sub>2</sub>X compounds. In our opinion, the results of Section 10 and the arguments in the present section contradict the concept of a well-defined superconducting pseudogap. However, we cannot casually dismiss the facts cited by the Orsay group—the significant magnetoresistance and the dependence of the electron contribution to the specific heat on the field in magnetic fields well below a threshold field, the rapid decrease in the temperature of the superconducting transition with the pressure (with moving away from the phase of the spin density wave), and, possibly, the particular sensitivity to defects.<sup>4)</sup> These points are difficult to explain without appealing to superconducting fluctuation phenomena of the paraconductivity type, and these phenomena would in turn probably result from a paramagnon mechanism. To what extent we could speak in terms of a triplet superconductivity here (i.e., an analogy with the A and B phases of <sup>3</sup>He) is still guesswork at this stage.

## 12. CONCLUSION

Here is a list of the physical phenomena and the problems which have arisen as a result of research on the (TMTSF)<sub>2</sub>X compounds:

1. The phase transitions in a magnetic field and the state of the spin density wave (Fig. 4). The explanation proposed in Section 8 is probably basically correct.

2. The fluctuational superconductivity. The discussion just above indicates an important role for the paramagnon mechanism and a relationship between superconductivity and antiferromagnetism in these compounds.

3. The discovery of a new type of structural transition in these compounds: an anionic ordering. The mechanism which controls these transitions is not clear at this point. For the low-temperature transitions, conduction electrons probably play a role in the energetics of the ordering. In turn, the ordering transitions determine the low-temperature properties of the electron subsystem.

4. The fact that slight external effects can put compounds with different anions—despite the broad variety of their initial properties—in a state in which the properties are essentially identical for all compounds and can be described by the phase diagram in Fig. 4. This assertion is subject to a more comprehensive experimental test.

5. The properties of the antiferromagnetic phase itself and the mechanism for its appearance (which have not been studied adequately).

The ideas which we have reviewed here require experimental tests. We believe that a crucial question for reaching

an understanding of this mechanism is the vector of the spin superstructure.

<sup>4)</sup>The absence of a residual-resistance regime can be attributed to the high purity of the materials. This regime appears in the Q state of (TMTSF)<sub>2</sub>ClO<sub>4</sub>.

- <sup>1</sup>K. Bechgaard, C. S. Jacobsen, K. Mortensen, H. J. Pedersen, and N. Thorup, *Solid State Commun.* **33**, 1119 (1980).  
<sup>2</sup>D. Jerome, A. Mazaud, M. Ribault, and K. Bechgaard, *J. Phys. Lett.* **41**, L-49 (1980).  
<sup>3</sup>W. A. Little, *Phys. Rev.* **A134**, 1416 (1964).  
<sup>4</sup>D. Jerome and H. J. Schulz, *Adv. Phys.* **31**, 299 (1982).  
<sup>5</sup>Colloque Intern. CNRS Phys. et Chim. Metaux Synthétiques et Organiques. *J. Phys. Coll. No. 3*, 1983.  
<sup>6</sup>R. Peierls, *Quantum Theory of Solids*, Clarendon Press, Oxford, 1955 (Russ. Transl., IL, M. 1956).  
<sup>7</sup>A. W. Overhauser, *Phys. Rev. Lett.* **4**, 507 (1960).  
<sup>8</sup>Yu. A. Bychkov, L. P. Gor'kov, and I. E. Dzyaloshinskii, *Pis'ma Zh. Eksp. Teor. Fiz.* **2**, 147 (1965) [*JETP Lett.* **2**, 92 (1965)]; *Zh. Eksp. Teor. Fiz.* **50**, 738 (1966) [*Sov. Phys. JETP* **23**, 489 (1966)].  
<sup>9</sup>I. E. Dzyaloshinskii and A. I. Larkin, *Zh. Eksp. Teor. Fiz.* **61**, 791 (1971) [*Sov. Phys. JETP* **34**, 422 (1972)].  
<sup>10</sup>J. Solovoy, *Adv. Phys.* **28**, 201 (1979).  
<sup>11</sup>L. P. Gor'kov and I. E. Dzyaloshinskii, *Zh. Eksp. Teor. Fiz.* **67**, 397 (1974) [*Sov. Phys. JETP* **40**, 198 (1975)].  
<sup>12</sup>L. P. Gor'kov, *Pis'ma Zh. Eksp. Teor. Fiz.* **34**, 602 (1981) [*JETP Lett.* **34**, 578 (1981)].  
<sup>13</sup>K. Bechgaard, K. Carneiro, M. Olsen, and F. B. Rasmussen, *Phys. Rev. Lett.* **46**, 852 (1981).  
<sup>14</sup>R. Brusetti, P. Garoche, and K. Bechgaard, *J. Phys. (Paris) CN3*, 1051 (1983).  
<sup>15</sup>J. F. Kwak, J. E. Schirber, R. L. Greene, and E. M. Engler, *Phys. Rev. Lett.* **46**, 1296 (1981).  
<sup>16</sup>J. F. Kwak, J. E. Schirber, R. L. Greene, and E. M. Engler, *Mol. Cryst. Liq. Cryst.* **79**, 111 (1982).  
<sup>17</sup>J. F. Kwak, *J. Phys. (Paris) CN3*, 839 (1983).  
<sup>18</sup>P. Garoche, R. Brusetti, D. Jerome, and K. Bechgaard, *J. Phys. Lett.* **43**, L-445 (1982).  
<sup>19</sup>T. Takahashi, D. Jerome, and K. Bechgaard, *J. Phys. Lett.* **43**, L-565, 805 (1982).  
<sup>20</sup>T. Takahashi, D. Jerome, and K. Bechgaard, *J. Phys. (Paris) CN3*, 805 (1983).  
<sup>21</sup>R. Brusetti, M. Ribault, D. Jerome, and K. Bechgaard, *J. Phys. (Paris) CN3*, 801 (1982).  
<sup>22</sup>C. S. Jacobsen, K. Mortensen, N. Thorup, D. B. Tanner, M. Weger, and K. Bechgaard, *Chem. Scripta* **17**, 103 (1981).  
<sup>23</sup>S. Barisic and S. Brazovskii, in: *Recent Developments in Condensed Matter Physics* (ed. J. T. Devreese), Vol. 1, Plenum Press, New York, p. 327.  
<sup>24</sup>C. S. Jacobsen, D. B. Tanner, and K. Bechgaard, *Phys. Rev. Lett.* **46**, 1142 (1981).  
<sup>25</sup>C. S. Jacobsen, D. B. Tanner, and K. Bechgaard, *J. Phys. (Paris) CN3*, 859 (1983).  
<sup>26</sup>S. S. P. Parkin, D. Jerome, and K. Bechgaard, *Mol. Cryst. Liq. Cryst.* **79**, 213 (1982).  
<sup>27</sup>R. Moret, J. P. Pouget, R. Comes, and K. Bechgaard, *J. Phys. (Paris) CN3*, 957 (1983).  
<sup>28</sup>K. Mortensen, C. S. Jacobsen, A. Lindegaard-Andersen, and K. Bechgaard, *J. Phys. (Paris) CN3*, 963 (1983).  
<sup>29</sup>J. P. Pouget, R. Moret, R. Comes, K. Bechgaard, J. M. Fabre, and L. Giral, *Mol. Cryst. Liq. Cryst.* **79**, 129 (1982).  
<sup>30</sup>R. Bruinsma and V. J. Emery, *J. Phys. (Paris) CN3*, 1115 (1983).  
<sup>31</sup>P. Delhaes, C. Coulon, J. Amiel, S. Flandrois, E. Torrelles, J. M. Fabre, and L. Giral, *Mol. Cryst. Liq. Cryst.* **50**, 43 (1979).  
<sup>32</sup>C. Coulon, P. Delhaes, S. Flandrois, R. Lagnier, E. Bonjour, and J. M. Fabre, *J. Phys. (Paris)* **43**, 1059 (1982).  
<sup>33</sup>S. S. P. Parkin, J. J. Mayerle, and E. M. Engler, *J. Phys. (Paris) CN3*, 1105 (1983).  
<sup>34</sup>S. Tomic, D. Jerome, P. Monod, and K. Bechgaard, *J. Phys. Lett.* **43**, L-839 (1982).  
<sup>35</sup>J. P. Pouget, G. Shirane, K. Bechgaard, and J. M. Fabre, *Phys. Rev.* **B27**, 5203 (1983).

- <sup>36</sup>T. Takahashi, D. Jerome, and K. Bechgaard, *J. Phys. Lett.* **43**, L-573, L-839 (1982).
- <sup>37</sup>S. Tomic, D. Jerome, and K. Bechgaard, *J. Phys. C* **17**, L11 (1984).
- <sup>38</sup>R. C. Lacoé, P. M. Chaikin, F. Wudl, and E. Aharon-Shalom, *J. Phys. (Paris) CN3*, 767 (1983).
- <sup>39</sup>J. M. Williams, M. A. Beno, J. C. Sullivan, L. M. Banovetz, J. M. Braam, G. S. Blackman, C. D. Carlson, D. L. Greer, D. M. Loesing, and K. Carneiro, *J. Phys. (Paris) CN3*, 941 (1983).
- <sup>40</sup>J. P. Puget, *Chem. Scripta* **17**, 85 (1981).
- <sup>41</sup>W. M. Walsh, F. Wudl, G. A. Thomas, D. Nalewajek, J. J. Hauser, P. A. Lee, and T. Poehler, *Phys. Rev. Lett.* **45**, 829 (1980).
- <sup>42</sup>H. J. Pedersen, J. C. Scott, and K. Bechgaard, *Solid State Commun.* **35**, 207 (1980).
- <sup>43</sup>J. C. Scott, H. J. Pedersen, and K. Bechgaard, *Phys. Rev. Lett.* **45**, 2125 (1980).
- <sup>44</sup>K. Mortensen, Y. Tomkiewicz, and K. Bechgaard, *Phys. Rev.* **B25**, 3319 (1982).
- <sup>45</sup>C. Kittel, *Quantum Theory of Solids*, Wiley, N. Y., 1963 (Russ. Transl., Nauka, M., 1967).
- <sup>46</sup>E. M. Lifshitz and L. B. Pitaevskii, *Statisticheskaya fizika (Statistical Physics)*, Part 2, Nauka, Moscow, 1978.
- <sup>47</sup>J. B. Torrance, H. J. Pedersen, and K. Bechgaard, *Phys. Rev. Lett.* **49**, 881 (1982).
- <sup>48</sup>W. M. Walsh, F. Wudl, E. Aharon-Shalom, L. W. Rupp, J. M. Vandenberg, K. Andres, and J. B. Torrance, *Phys. Rev. Lett.* **49**, 885 (1982).
- <sup>49</sup>S. S. P. Parkin, J. C. Scott, J. B. Torrance, and E. M. Engler, *Phys. Rev.* **B26**, 6319 (1982).
- <sup>50</sup>J. C. Scott, H. J. Pedersen, and K. Bechgaard, *Phys. Rev.* **B24**, 475 (1981).
- <sup>51</sup>A. Andrieux, D. Jerome, and K. Bechgaard, *J. Phys. Lett.* **42**, L-871 (1981).
- <sup>52</sup>C. S. Jacobsen, K. Mortensen, M. Weger, and K. Bechgaard, *Solid State Commun.* **38** 423 (1981).
- <sup>53</sup>B. Horovitz, H. Gutfreund, and M. Weger, *Mol. Cryst. Liq. Cryst.* **79**, 591 (1982).
- <sup>54</sup>B. Horovitz, H. Gutfreund, and M. Weger, *Phys. Rev.* **B12**, 3174 (1975).
- <sup>55</sup>L. V. Keldysh and Yu. V. Kopaev, *Fiz. Tverd. Tela (Leningrad)* **6**, 2791 (1964) [*Sov. Phys. Solid State* **6**, 2219 (1964)].
- <sup>56</sup>T. Takahashi, F. Creuzet, D. Jerome, and J. M. Fabre, *J. Phys. (Paris) CN3*, 1095 (1983).
- <sup>57</sup>H. J. Schulz and D. Jerome, *J. Phys. (Paris)* **42**, 991 (1981).
- <sup>58</sup>D. Jerome, *Mol. Cryst. Liq. Cryst.* **79**, 155 (1982).
- <sup>59</sup>A. Andrieux, C. Duroure, D. Jerome, and K. Bechgaard, *J. Phys. Lett.* **40**, L-381 (1979).
- <sup>60</sup>H. J. Schulz, D. Jerome, A. Mazaud, M. Ribault, and K. Bechgaard, *J. Phys. (Paris)* **42**, 991 (1981).
- <sup>61</sup>P. M. Chaikin, M. Y. Choi, P. Haen, E. M. Engler, and R. L. Greene, *Mol. Cryst. Liq. Cryst.* **79**, 435 (1982).
- <sup>62</sup>P. M. Chaikin, M. Y. Choi, and R. L. Greene, *J. Phys. (Paris) CH3*, 783 (1983).
- <sup>63</sup>R. Brusetti, K. Bechgaard, G. G. Lonzarich, and R. H. Friend, *J. Phys. (Paris) CH3*, 1055 (1983).
- <sup>64</sup>K. Kajimura, H. Tokumoto, M. Tokumoto, K. Murata, T. Ukachi, H. Anzai, T. Ishiguro, and G. Saito, *J. Phys. (Paris) CH3*, 1059 (1983).
- <sup>65</sup>J. F. Kwak, *Phys. Rev.* **B28**, 3277 (1983).
- <sup>66</sup>P. Garoche, R. Brusetti, D. Jerome, and K. Bechgaard, *J. Phys. Lett.* **43**, L-147 (1982).
- <sup>67</sup>R. Brusetti, P. Garoche, and K. Bechgaard, *J. Phys. C* **16**, 3535 (1983).
- <sup>68</sup>L. J. Avezedo, J. E. Schierber, R. L. Greene, and E. M. Engler, *Physica B108*, 1183 (1981).
- <sup>69</sup>M. Ribault, D. Jerome, J. Tuchendler, C. Weyl, and K. Bechgaard, *J. Phys. Lett.* **44**, L-953 (1983).
- <sup>70</sup>P. M. Chaikin, M. Y. Choi, J. F. Kwak, J. S. Brooks, K. P. Martin, M. J. Naughton, E. M. Engler, and R. L. Greene, *Phys. Rev. Lett.* **51** 2333 (1983).
- <sup>71</sup>K. Klitzing, G. Dorda, and M. Pepper, *Phys. Rev. Lett.* **45**, 494 (1980).
- <sup>72</sup>L. P. Gor'kov and A. G. Lebed', *J. Phys. Lett.* **45**, 433 (1984).
- <sup>73</sup>D. Jerome, *J. Phys. (Paris) CN3*, 775 (1983).
- <sup>74</sup>L. P. Gor'kov and T. T. Mnatsakanov, *Zh. Eksp. Teor. Fiz.* **63**, 684 (1972) [*Sov. Phys. JETP* **36**, 361 (1973)].
- <sup>75</sup>S. A. Brazovskii, I. E. Dzyaloshinskii, and N. N. Kirova, *Zh. Eksp. Teor. Fiz.* **81**, 2279 (1981) [*Sov. Phys. JETP* **54**, 1209 (1981)].
- <sup>76</sup>S. A. Brazovskii, L. P. Gor'kov, and A. G. Lebed', *Zh. Eksp. Teor. Fiz.* **83**, 1198 (1982) [*Sov. Phys. JETP* **56**, 683 (1982)].
- <sup>77</sup>H. J. Schulz and C. Bourbonnais, *Phys. Rev.* **B27**, 5856 (1983).
- <sup>78</sup>H. J. Schulz, *J. Phys. (Paris) CN3*, 903 (1983).
- <sup>79</sup>C. Bourbonnais and L. G. Caron, *J. Phys. (Paris) CN3*, 911 (1983).
- <sup>80</sup>L. Forro, K. Biljakovic, J. R. Cooper, and K. Bechgaard, *Phys. Rev.* **B29**, 2839 (1984).
- <sup>81</sup>M. Y. Choi, P. M. Chaikin, and R. L. Greene, *J. Phys. (Paris) CN3*, 1067 (1983).
- <sup>82</sup>D. Djurek, M. Preseter, D. Jerome, and K. Bechgaard, *J. Phys. C* **15**, L-669 (1982).
- <sup>83</sup>D. Djurek, D. Jerome, and J. Bechgaard, *J. Phys. C* **17**, 4179 (1984).
- <sup>84</sup>C. More, G. Roger, J. P. Sorbier, D. Jerome, M. Ribault, and K. Bechgaard, *J. Phys. Lett.* **42**, L-313 (1981).
- <sup>85</sup>A. Fournel, C. More, G. Roger, J. P. Sorbier, J. M. Delrieu, D. Jerome, M. Ribault, and K. Bechgaard, *J. Phys. Lett.* **42**, L-445 (1981).
- <sup>86</sup>A. Fournel, C. More, G. Roger, *et al.*, *J. Phys. (Paris) CN3*, 879 (1983).
- <sup>87</sup>H. K. Ng, T. Timusk, J. M. Delrieu, D. Jerome, K. Bechgaard, and J. M. Fabre, *J. Phys. Lett.* **43**, L-513 (1982).
- <sup>88</sup>H. K. Ng, T. Timusk, and K. Bechgaard, *J. Phys. (Paris) CN3*, 867 (1983).
- <sup>89</sup>W. A. Challener, P. L. Richards, and R. L. Greene, *J. Phys. (Paris) CN3*, 873 (1983).
- <sup>90</sup>C. S. Jacobsen, D. B. Tanner, and K. Bechgaard, *J. Phys. (Paris) CN3*, 859 (1983).
- <sup>91</sup>C. S. Jacobsen, D. B. Tanner, and K. Bechgaard, *Phys. Rev.* **B28**, 7019 (1983).
- <sup>92</sup>E. H. Lieb and F. Y. Wu, *Phys. Rev. Lett.* **20**, 1445 (1968).
- <sup>93</sup>A. A. Ovchinnikov, *Zh. Eksp. Teor. Fiz.* **57**, 2137 (1969) [*Sov. Phys. JETP* **30**, 1160 (1970)].
- <sup>94</sup>P. M. Grant, *J. Phys. (Paris) CN3*, 847 (1983).
- <sup>95</sup>M. Weger and H. Gutfreund, *Commun. Solid State Phys.* **8**, 135 (1978).
- <sup>96</sup>L. P. Gor'kov, E. N. Dolgov, and A. G. Lebed', *Zh. Eksp. Teor. Fiz.* **82**, 613 (1982) [*Sov. Phys. JETP* **55**, 365 (1982)].
- <sup>97</sup>L. G. Aslamazov and A. I. Larkin, *Fiz. Tverd. Tela (Leningrad)* **10**, 1104 (1968) [*Sov. Phys. Solid State* **10**, 875 (1968)].

Translated by Dave Parsons